Report No. FAA-RD-74-137

FAA WJH Technical Center
00026720

TECHNICAL EVALUATION OF WEATHER CLUTTER FEASIBILITY MODEL

Ronald S. Bassford

SEPTEMBER 1974

FINAL REPORT

Document is available to the public through the
National Technical Information Service,
Springfield, Virginia 22151

Prepared for

U.S. DEPARTMENT OF TRANSPORTATION
FEDERAL AVIATION ADMINISTRATION
Systems Research & Development Service
Washington, D. C. 20590

NOTICE

This document is disseminated under the sponsorship of the Department of Transportation in the interest of information exchange. The United States Government assumes no liability for its contents or use thereof.

F.A.A., National Aviation Facilities Experimental Center
Technical Evaluation of Weather Clutter Feasibility Model, by Ronald S. Bassford. Final report. Atlantic City, N.J., September 1974.

70 p. (RD-74-137)
(NA-74-25)
Project No. 022-242-010

1. Weather--Display System-Testing. 2. Weather Clutter. 3. ASR-5. Models. I. Bassford, Ronald S.

Technical Report Documentation Page

1. Report No.	2. Government Accession No.	3. Recipient's Catalog No.
FAA-RD-74-137		

4. Title and Subtitle	5. Report Date
TECHNICAL EVALUATION OF WEATHER CLUTTER FEASIBILITY MODEL	September 1974
	6. Performing Organization Code
7. Author(s) Ronald S. Bassford	8. Performing Organization Report No. FAA-NA-74-25
9. Performing Organization Name and Address Federal Aviation Administration National Aviation Facilities Experimental Center Atlantic City, New Jersey 08405	10. Work Unit No. (TRAIS) 11. Contract or Grant No. 022-242-010
12. Sponsoring Agency Name and Address U.S. Department of Transportation Federal Aviation Administration Systems Research and Development Service Washington, D.C. 20590	13. Type of Report and Period Covered Final June 1970 - June 1974 14. Sponsoring Agency Code

15. Supplementary Notes

16. Abstract

An ASR-5 weather clutter feasibility model was developed and evaluated to determine its capability to provide air traffic controllers with a weather display (clutter free) of air traffic and a contour depiction of weather detected by radar. The technical tests included the determination of technical characteristics of each of four modifications (narrow transmitter pulse width, noncoherent moving target indicator, dual frequency diversity, and logarithmic/fast time constant) which comprised the weather rejection portion of the system along with their capabilities to provide clutter rejection and target detection in weather. The four modifications were then tested in unison to determine the system's overall capability. The weather channel portion of the equipment was tested to determine its capability to provide weather clutter formatting in the form of isoamplitude contours. The results of the test demonstrated that the weather clutter feasibility model does not effectively perform the designed functions of weather clutter rejection and weather clutter contouring. Its capability to provide weather clutter contouring ranges from good, for high-level well defined weather cells, to poor, for low-level scattered cells. The equipment is not acceptable for use in the air traffic control system.

17. Key Words	18. Distribution Statement
Weather Clutter Rejection Weather Clutter Contouring Airport Surveillance Radar Air Traffic Control	Document is available to the public through the National Technical Information Service, Springfield, Virginia 22151

19. Security Classif. (of this report)	20. Security Classif. (of this page)	21. No. of Pages	22. Price
Unclassified	Unclassified	70	

Form DOT F 1700.7 (8-72) Reproduction of completed page authorized

TABLE OF CONTENTS

	Page
INTRODUCTION	1
Purpose	1
Background	1
Description of Equipment	1
Discussion	1
TEST PROCEDURES AND RESULTS	2
Reduced Transmitter Pulse Width	2
Noncoherent MTI	4
Dual Frequency Diversity	10
Logarithmic Amplifier/Fast Time Constant (Log/FTC)	17
Weather Channel	27
Overall System Tests	31
Modified ASR-7 Weather Tests	46
SUMMARY OF RESULTS	50
CONCLUSIONS	52
RECOMMENDATION	52
REFERENCES	52
APPENDIXES	
A Description of Modified ASR-5	
B Equipment Modifications	
C Special Test Equipment	

LIST OF ILLUSTRATIONS

Figure		Page
1	ASR-5 Transmitter Pulse Width Comparison Standard Versus Narrow	3
2	Target Detection Capability - Standard (Channel A) Versus Narrow (Channel B) Pulse Width	5
3	Noncoherent IF Amplifier Target Attenuation Versus Clutter Signal Amplitude	7
4	Coherent/Noncoherent MTI Clutter Gating (10-Mile Range Marks)	9
5	Noncoherent MTI Clutter Attenuation (10-Mile Range Marks)	11
6	Noncoherent MTI Target Detection (5-Mile Range Marks)	12
7	Frequency Diversity Combiner Performance	14
8	MTI Multiplicative Combining, Probability of Detection	16
9	Additive Combining, Weather Clutter and Noise Decorrelation	16
10	Frequency Diversity Clutter Rejection	18
11	Log/FTC Circuit Block Diagram	20
12	Log Amplifier Transfer Characteristics	21
13	Log Amplifier Input Versus RF Signal Strength	22
14	Log/FTC Superclutter Visibility of a Ring-Around Target	24
15	Log/FTC Superclutter Visibility of an Azimuth-Modulated Target	25
16	Log/FTC Residue	26
17	Log/FTC Residue and Blackholing	28
18	Weather Channel Simplified Block Diagram	29
19	System Weather Clutter Rejection (10-Mile Range Marks and 35-dB Weather)	32
20	System Weather Clutter Rejection (10-Mile Range Marks and 35-dB Weather)	33

LIST OF ILLUSTRATIONS (continued)

Figure		Page
21	Combined Log/FTC and Frequency Diversity Weather Clutter Rejection (10-Mile Range Marks)	35
22	Combined Noncoherent MTI and Frequency Diversity Weather Clutter Rejection (10-Mile Range Marks)	36
23	Combined Noncoherent MTI and Log/FTC Weather Clutter Rejection (10-Mile Range Marks)	37
24	System Weather Clutter Rejection (5-Mile Range Marks and 30-dB Weather)	39
25	System Weather Clutter Rejection (10-Mile Range Marks and 24-dB Weather)	40
26	System Target Detection (10-Mile Range Marks and 30-dB Weather)	41
27	System Target Detection (10-Mile Range Marks and 15-dB Weather)	43
28	System Target Detection (10-Mile Range Marks and 15-dB Weather)	44
29	Aircraft Tracks	45
30	ASR-7 Weather Modification	47
31	Modified ASR-7 Test Target Detection in Weather	48
32	Relative Subclutter Visibilities of Modified ASR-7 Videos	49
A-1	Weather Clutter Feasibility Model Equipment	A-2
A-2	Weather Clutter Feasibility Model Simplified Block Diagram	A-3

INTRODUCTION

PURPOSE.

The purpose of this project was to determine the capability of a weather clutter rejection and contouring subsystem which was designed to improve operation of the existing airport surveillance radar (ASR-5).

BACKGROUND.

Under FAAR 6420.1, dated November 1966, a system requirement was levied for the development of techniques and equipment which would eliminate weather clutter video from the terminal-radar environment. In response to this requirement, the Federal Aviation Administration (FAA) Systems Research and Development Service awarded a contract (FA69WA-2107) on July 10, 1969, to Texas Instruments Inc. for the design, development, and fabrication of an ASR-5 weather clutter feasiblility model. The contract specified that the model should also include the capability of generating up to two levels of weather contours for use by air traffic control specialists (ATCS) in the identification of areas of precipitation. The feasibility model was delivered to the National Aviation Facilities Experimental Center (NAFEC) for evaluation.

Subsequent to the original test effort of evaluating the weather clutter feasibility model, the noncoherent MTI log/FTC concept was investigated further at the NAFEC ASR-7 site.

DESCRIPTION OF EQUIPMENT.

To achieve a minimum objective of an additional 10 decibels (db) of weather clutter rejection, the ASR-5 system was modified to include the following four techniques for clutter rejection:

1. Reduced Transmitter Pulse Width.
2. Noncoherent Moving Target Indicator (MTI).
3. Video Logarithmic Fast Time Constant (Log/FTC).
4. Dual Frequency Diversity.

Also, a separate receiving channel was provided for weather detection. A description of each of the above modifications is included under the appropriate testing section. Further details and equipment photographs are contained in appendix A, Description of Modified ASR-5.

DISCUSSION.

The four weather modification equipment fixes for reducing weather clutter on a plan position indicator (PPI) can be used singly or together. Therefore, each fix was examined separately to determine its characteristics and capability, and then the overall system was tested for clutter rejection.

Concurrently with the above testing, the weather-contouring channel was examined to determine its capability to provide weather-clutter gating to the noncoherent MTI and to provide retrieval of weather clutter in the form of contours.

TEST PROCEDURES AND RESULTS

REDUCED TRANSMITTER PULSE WIDTH.

The radar cell volume is a function of the transmitted pulse width and the half-power beamwidth of the antenna. Since a weather clutter cell is normally equivalent to this radar cell volume (whereas a target may occupy only a portion of this total volume), a reduction in transmitted pulse width would improve the probability of detecting a target in areas of weather clutter (reference 1). Therefore, to obtain a 50-percent reduction in transmitter pulse width and the resulting 3-dB reduction in clutter echo power, the ASR-5 transmitter was modified by replacement of the pulse-forming network, pulse transformer, and despiking network. Also, the DX-276 magnetron was replaced with a JAN 5586 type, capable of handling the doubled peak power output necessary for maintaining the same average power output for target detection. Initially, only one of the two ASR-5 channels (channel B) was modified so that comparison data could be collected concurrently from both modified and unmodified channels. Data collection and analysis of the design were directed towards determining (1) measurement of pulse width reduction to enable calculating the degree of reduction in weather clutter power, and (2) target detection capability based on actual tracking of an aircraft in areas that were clear of weather clutter.

PULSE WIDTH CHARACTERISTICS. Since the theoretical 3-dB reduction in clutter echo power was based on a 50-percent reduction in transmitter pulse width, measurement of the transmitted pulse width of both the modified and unmodified channels was necessary to ascertain the degree of reduction of clutter echo power.

For each channel, the signal available at the directional coupler was attenuated and coupled to a crystal detector to enable the display of the transmitted pulse on a Tektronix 545A oscilloscope. Figure 1, which depicts the detected envelope of the pulse from each channel, was used to ascertain the pulse width of the modified and unmodified channels. Note that the pulse width was measured at the half-power points (0.707 on the voltage envelope) since this is the point of reference for the pulse width parameter in the radar range equation (reference 1).

Figure 1 shows a pulse width of 0.78 microseconds (μs) for channel A and 0.4 μs for channel B. This ratio of 1.95/1 approximates the desired 3-dB design factor for reduction of weather clutter power.

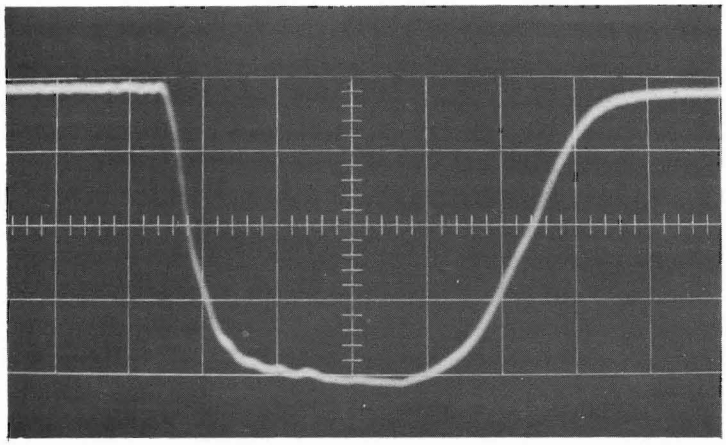

(a) STANDARD ASR-5 TRANSMITTER PULSEWIDTH (0.2 μs/cm)

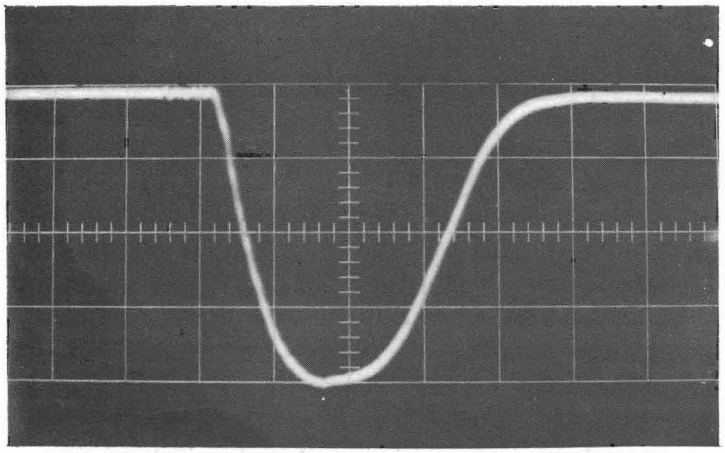

(b) NARROW TRANSMITTER PULSEWIDTH (0.2 μs/cm)

FIGURE 1. ASR-5 TRANSMITTER PULSE WIDTH COMPARISON STANDARD VERSUS NARROW

TARGET DETECTION. A 3-dB reduction in clutter echo power can be considered significant if target detection is not degraded as a result of reducing the pulse width. Although the transmitter peak power was doubled to maintain the same average power output, a flight test was made to ascertain the target-detection capabilities of the modified and unmodified channels.

The dual diversity aspect of the ASR-5 weather modification enabled display of video from channel A and delayed video from channel B (narrow pulse), concurrently, on a single UPA-35 PPI. An aircraft-tracking gate (part of the NAFEC radar test bed) was available to assure identification of a test aircraft (Aerocommander) proceeding outbound and inbound along a radial of the ASR-5 facility at an altitude of 6,000 feet. PPI photographic data, of normal video taken every other antenna scan to determine the percentage of scans (blip/scan ratio) in which the aircraft was detected, are depicted in a series of sample photographs shown in figure 2. In this figure, the target nearest to the radar origin is that obtained from channel A and the delayed target is that from channel B. For data collection purposes, loss of target on either channel was recorded on each scan whenever it was not visible, or was noticeably weaker than the target from the other channel. The receiver bandwidths were not changed when the transmitters were modified for narrow-pulse operation.

For 727 scans of data, and when the aircraft was between 30 nautical miles and maximum radar range (loss of target), the blip/scan ratio was 71.3 percent for channel A and 70.4 percent for channel B. For radar ranges less than 30 nautical miles, the blip/scan ratio was essentially 100 percent for both channels. The less than 1-percent difference between the blip/scan ratios of the two channels indicates that the target detection capability of the modified channel was not significantly degraded as a result of the reduced pulse width.

Small system gain variations between ASR-5 radar channels and the difficulty of determining a 3-dB reduction in clutter on a PPI presentation made determining the actual target visibility in weather clutter improvement beyond the scope of this project.

NONCOHERENT MTI.

The theory of noncoherent MTI is discussed in the literature (references 1 and 2). A brief summary is included here to complement the following discussion. Noncoherent MTI detects targets by the relative motion between the targets and a clutter background. This is done by using envelope-detected video as the input to the MTI canceller circuits, with clutter providing the reference signal for moving-target detection. The radial component of the relative motion of the target to clutter produces the necessary Doppler beat. Since noncoherent MTI uses envelope detection, it is not sensitive to slight changes in carrier frequency. It, therefore, removes the mean velocity component due to wind leaving only clutter fluctuations and MTI passband shape as limiting factors in clutter attenuation. However, signals must not be amplitude limited. Since noncoherent MTI depends upon the beat between targets and clutter, it cannot detect targets in the clear. Therefore, means must be provided to use noncoherent MTI only in clutter areas. Both blind speeds and blind phases exist when using noncoherent MTI.

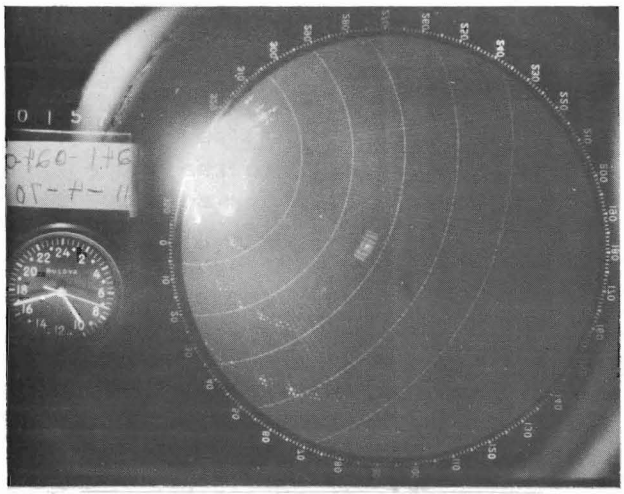

(a) CHANNEL B TARGET DISPLAYED

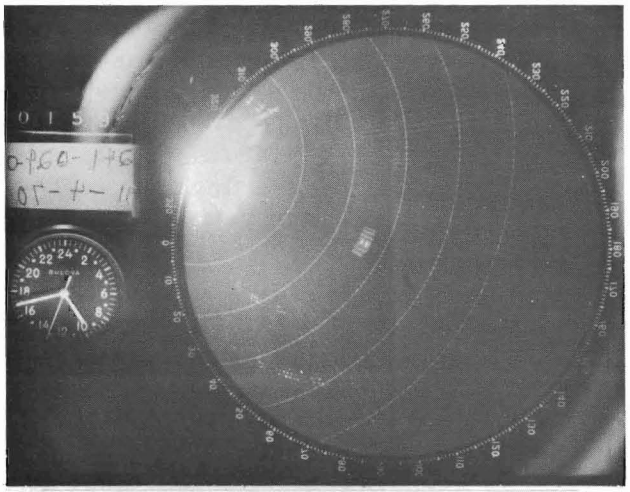

(b) BOTH CHANNELS TARGETS DISPLAYED

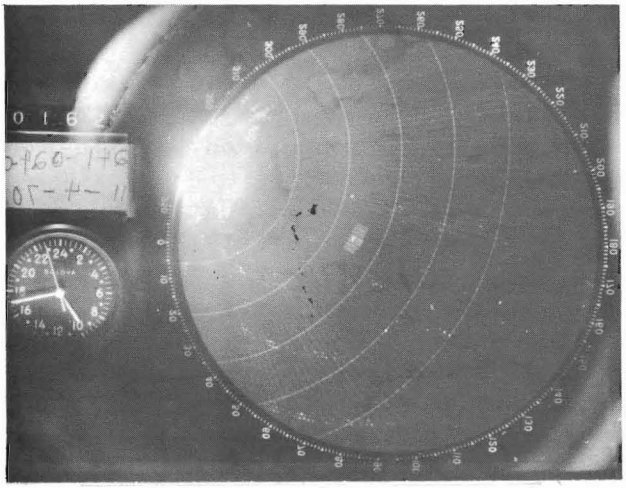

(c) CHANNEL A TARGET DISPLAYED

FIGURE 2. TARGET DETECTION CAPABILITY - STANDARD (CHANNEL A) VERSUS NARROW (CHANNEL B) PULSE WIDTH

CIRCUIT DESCRIPTION. The noncoherent MTI portion of the weather modification equipment consisted of a linear envelope-detecting intermediate frequency (IF) amplifier and associated clutter gate for each of the ASR-5 channels. Signals from the ASR-5 preamps were fed to the noncoherent IF amplifiers for amplitude detection. The clutter gates selected either this video or coherent video from the ASR-5 MTI IF amplifiers for application to the canceller circuits. This switching could be accomplished automatically or manually. In automatic operation, clutter-gating signals from the weather channel gated through noncoherent MTI video only when clutter was present. In manual operation, the video to the cancellers could be selected to be either all noncoherent MTI or all coherent MTI. Gain controls associated with each IF amplifier enabled matching the noncoherent MTI and coherent MTI video levels. One of four sensitivity time control (STC) curves for application to the noncoherent MTI IF amplifiers could be selected by a front panel switch. Since the clutter gates were initiated by the weather channel, the areas in which noncoherent MTI video was displayed corresponded to those enclosed by contours. To prevent clutter gating on aircraft target returns, which would result in the loss of aircraft returns in the clear, a modification was made to the contouring circuitry (see appendix B). Unless otherwise indicated, clutter gating signals (and contours) were developed by using ASR-5 channel A IF receiver signals as inputs to the weather channel IF amplifiers. This was necessitated by the lack of weather signals intense enough to provide the circular polarizer punchthrough required for total weather receiver operation.

CIRCUIT TESTS. The IF amplifiers, clutter gates, and STC functions were examined to determine their characteristics.

IF Amplifiers. The IF amplifiers were tested for sensitivity, dynamic range, and ability to handle large clutter signals without saturating.

Sensitivity was determined by standard minimum discernible signal (MDS) techniques. Both amplifiers provided sensitivities of -110 dBm (equal to that at the output of the ASR-5 normal IF amplifiers).

Dynamic range was determined by measuring the difference in the signal generator outputs necessary to produce MDS and limit level signals at the amplifier outputs. Both amplifiers provided dynamic ranges of 35 dB.

It was noted during the test period that ground clutter and large weather cells caused saturation of the IF amplifiers, and consequently, loss of sensitivity and improper video levels to the ASR-5 cancellers. Tests were conducted to determine the relationship between clutter strength and loss of sensitivity. A simulated target signal from an S-band signal generator and simulated clutter from a noise source (140 μs in duration) were introduced simultaneously into the system. The target signal strength out of the IF amplifier was then recorded as the clutter level was increased. Figure 3 is a graph of target attenuation as a function of clutter strength for this particular clutter signal. Since this type of saturation is a function of clutter duration as well as amplitude, target attenuation would also depend on the duration of individual weather signals. Figure 3 shows that simulated large blocks of weather clutter seriously degraded operation of the noncoherent MTI.

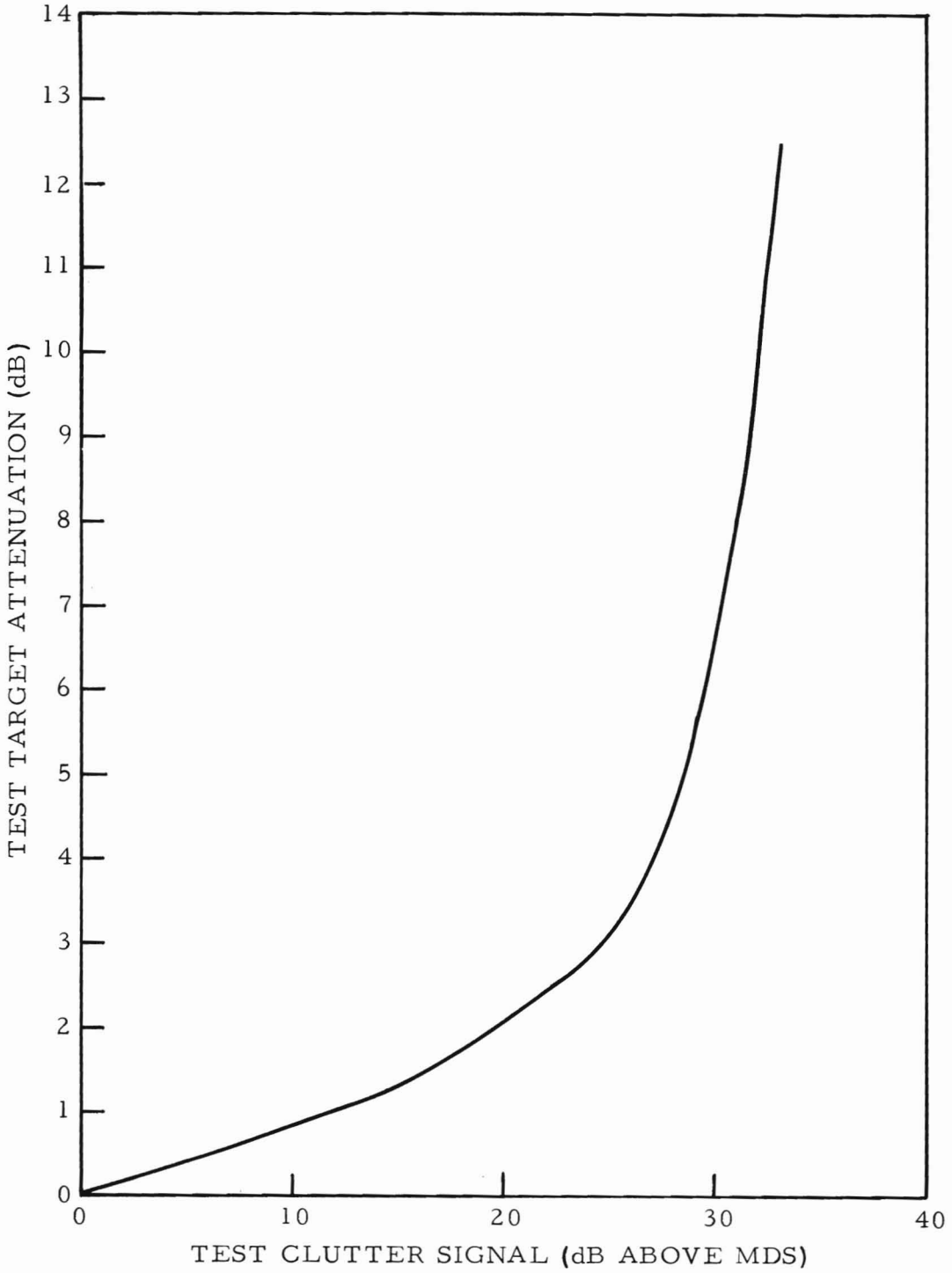

FIGURE 3. NONCOHERENT IF AMPLIFIER TARGET ATTENUATION VERSUS CLUTTER SIGNAL AMPLITUDE

Clutter Gates. The clutter gates were examined to determine their ability to gate in noncoherent MTI video for areas of weather. This was done by photographing and comparing the PPI presentation of weather signals, the corresponding contours, and the clutter-gated noncoherent/coherent MTI video. An example of this is shown in figure 4. The weather cell shown had a maximum intensity of 24 dB above system noise level. The leading edge of the weather (to the right of the photograph) had a steep gradient resulting in a fairly regular contour. The trailing edge gradient, being gradual, resulted in poor contouring. Since the noncoherent/coherent clutter gating was controlled by the contour signals, the contouring irregularities were directly related to clutter gating irregularities as seen in figure 4. The clutter gating ranged from good, for high-level well defined weather cells, to poor, for low-level scattered weather cells. The clutter gate switching action added to display residue as discussed below. As shown in figure 4(b), contouring began approximately 2 miles from the radar origin. This was due to the timing of the contouring circuitry. Since the clutter gates were derived from the contours, coherent MTI video was displayed within 2 miles. Other clutter was also present in figure 4(c), which was not due to clutter gating (not directly related to the contours shown in figure 4(b)). This additional clutter was due to internal weather clutter motion and to the Doppler beat between the ground clutter and the weather as discussed below.

Sensitivity Time Control Operation. Sensitivity time control action for the noncoherent IF amplifiers was obtained by coupling the weather channel STC voltage to each amplifier by means of an STC buffer amplifier. These units had gain, balance, and attenuation controls for setting the desired levels. Correct operation was verified by introducing an S-band test signal into an ASR-5 directional coupler and noting its attenuation as a function of time at the IF amplifier output.

WEATHER REJECTION. The noncoherent MTI was tested for subclutter visibility and for clutter residue.

Subclutter Visibility. The maximum subclutter visibility of noncoherent MTI approximates the subclutter visibility of the associated MTI canceller system (reference 1). To verify this for the equipment under test, the output of a S-band signal generator was introduced into an ASR-5 directional coupler and positioned so as to be superimposed on weather signals observed on the PPI. The difference between the amplitude of the weather signals and that of the test signal necessary to be barely discernible in the weather when using noncoherent MTI was considered to be the subclutter visibility. Approximately 20 dB of subclutter visibility was obtained. Target detection was improved in direct correspondence to the amount of weather clutter reduction. Thus, for the particular case discussed above, the 21 dB of weather reduction resulted in approximatley 21 dB of increased subclutter visibility. However, as shown in figure 3, noncoherent MTI IF amplifier saturation caused attenuation of target signals as a function of clutter signal strength. This precluded an exact determination of target detection in weather improvement.

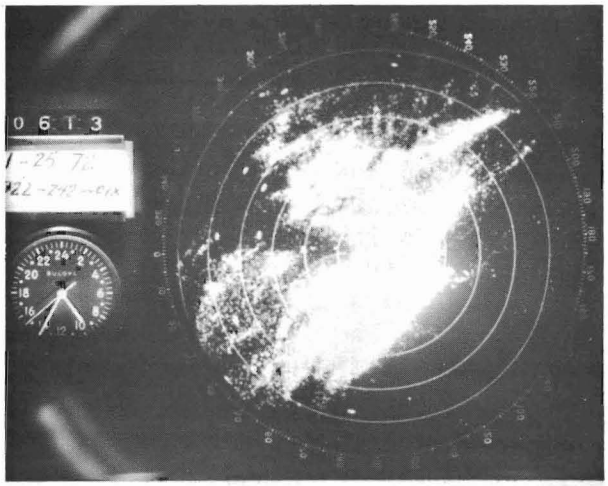

(a) COHERENT MTI VIDEO

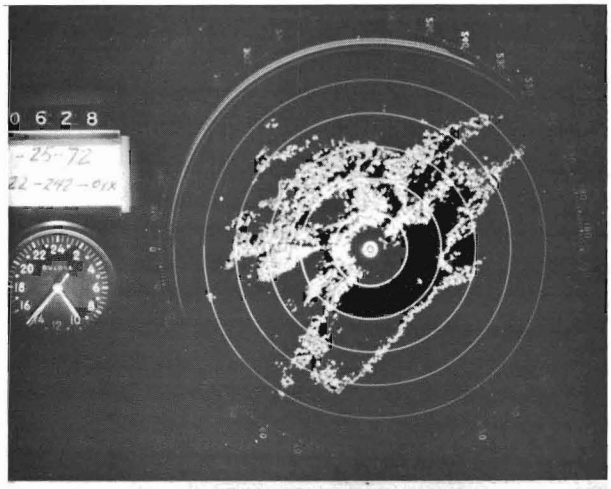

(b) CONTOURS

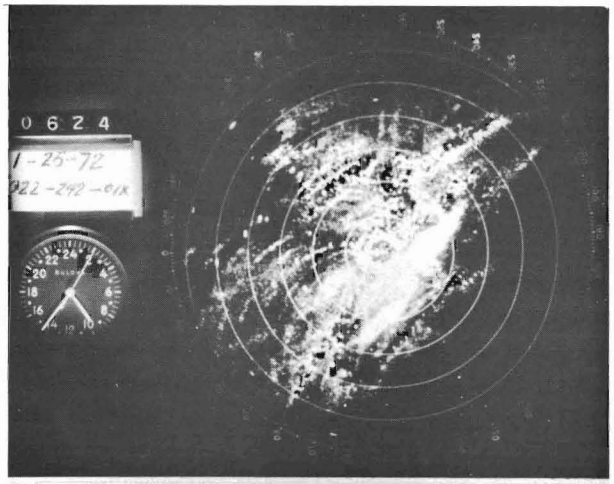

(c) CLUTTER GATED
COHERENT - NONCOHERENT MTI VIDEO

FIGURE 4. COHERENT/NONCOHERENT MTI CLUTTER GATING (10-MILE RANGE MARKS)

Weather Residue. Figures 4 and 5 illustrate the weather rejection capability of the noncoherent MTI system. In figure 5, the coherent MTI presentation of a weather cell 30 dB in intensity is shown along with the same cell displayed using noncoherent MTI in the manual (ungated) mode. Using this mode of operation, up to 21 dB of additional weather rejection was obtained. The weather rejection capability was determined by inserting a variable attenuator in the coherent MTI IF signal line. The attenuator was adjusted to reduce the coherent MTI clutter level to be equal to that of the noncoerent MTI as viewed on the system PPI. This amount of attenuation was, therefore, equal to the noncoherent MTI weather rejection capability. Since noncoherent MTI has clutter fluctuation limitations, this figure varied for individual weather cells. Figure 4 shows the same type of residue for the intense portion of the weather along with the residue generated by the gating action. Portions of the weather cell which were below the clutter gating level were displayed as coherent MTI. The switching from coherent to noncoherent MTI video created the type of residue pattern shown. The noncoherent MTI weather residue area in figure 5(b) extended to the 20-mile range mark on the average. This was approximately twice as far as the ground clutter extended. Therefore, the limiting factor in noncoherent MTI weather rejection, in this instance, was internal weather clutter motion and not the Doppler beat between the weather and the land clutter. The intense portion of the weather shown in figure 4(c) was over an area devoid of ground clutter and was due entirely to weather clutter fluctuations.

TARGET DETECTION. The noncoherent MTI provided greater target visibility in weather clutter than was obtained with coherent MTI. In figure 5, aircraft are visible using noncoherent MTI which were masked by the coherent MTI residue. Figure 6 shows a similar instance using gated noncoherent MTI video. Two aircraft, one at 330° and 9.5 miles and the other at 205° and 7.5 miles are visible using noncoherent operation. The targets shown were in 15 dB of weather.

However, the portion of the weather cells that the noncoherent MTI didn't eliminate and the gating residue limited target detection as can be seen in figures 4 and 6.

DUAL FREQUENCY DIVERSITY.

The two channels of the ASR-5 were configured to operate, in synchronism, at a frequency separation of 85 MHz. With channel B delayed during transmission and realigned to channel A after reception, video from both channels was combined to improve system performance in detecting targets in areas of weather clutter. This improvement was due to the decorrelation of weather clutter video from the two radar channels caused by the noiselike and frequency sensitive nature of weather clutter signals. This decorrelation resulted in a lessening of clutter signal strength at the output of the combiners (references 1 and 3).

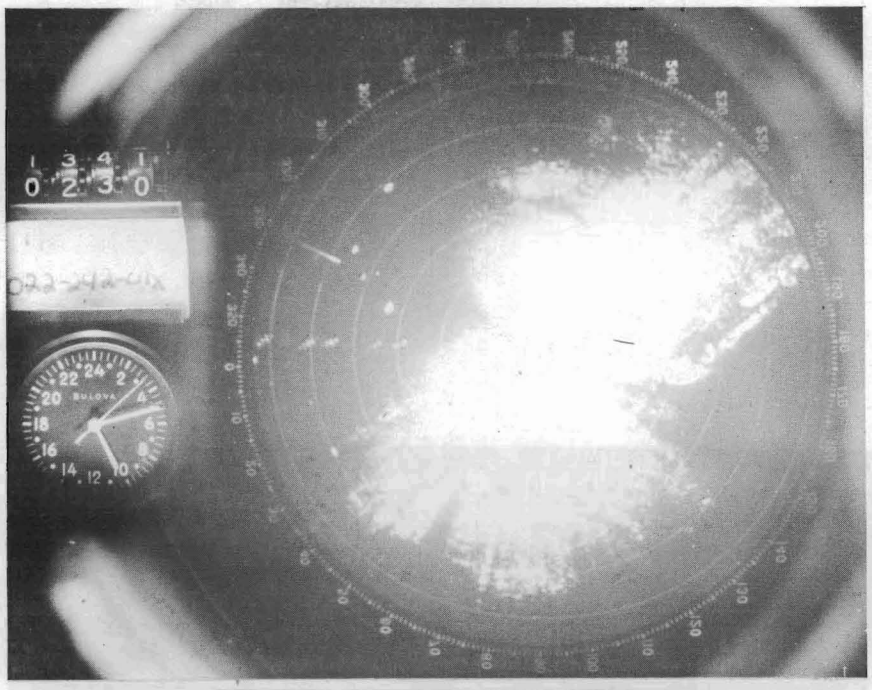

(a) COHERENT MTI VIDEO

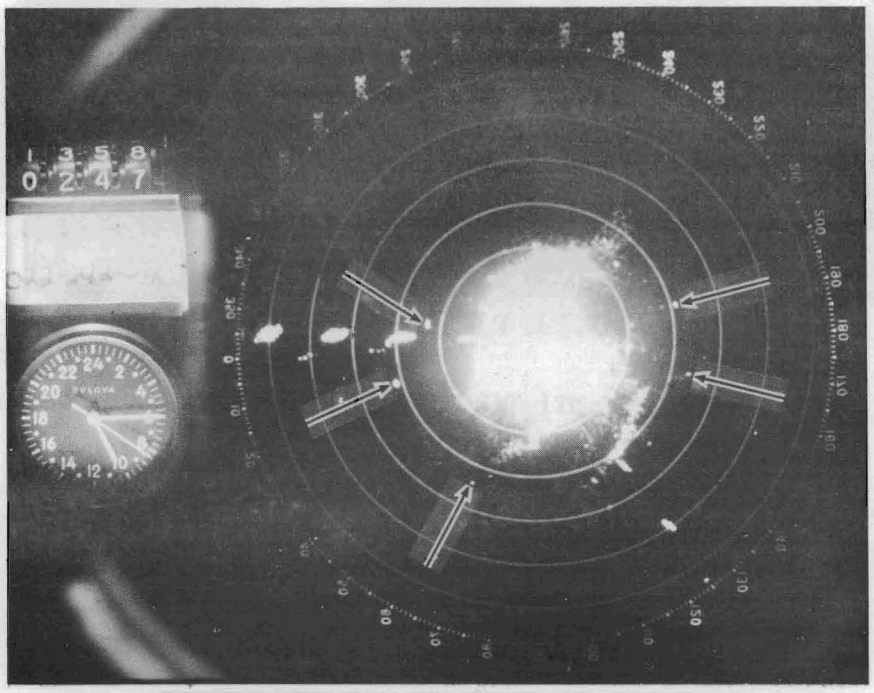

(b) NONCOHERENT MTI VIDEO

(ARROWS INDICATE AIRCRAFT SIGNALS)

FIGURE 5. NONCOHERENT MTI CLUTTER ATTENUATION (10-MILE RANGE MARKS)

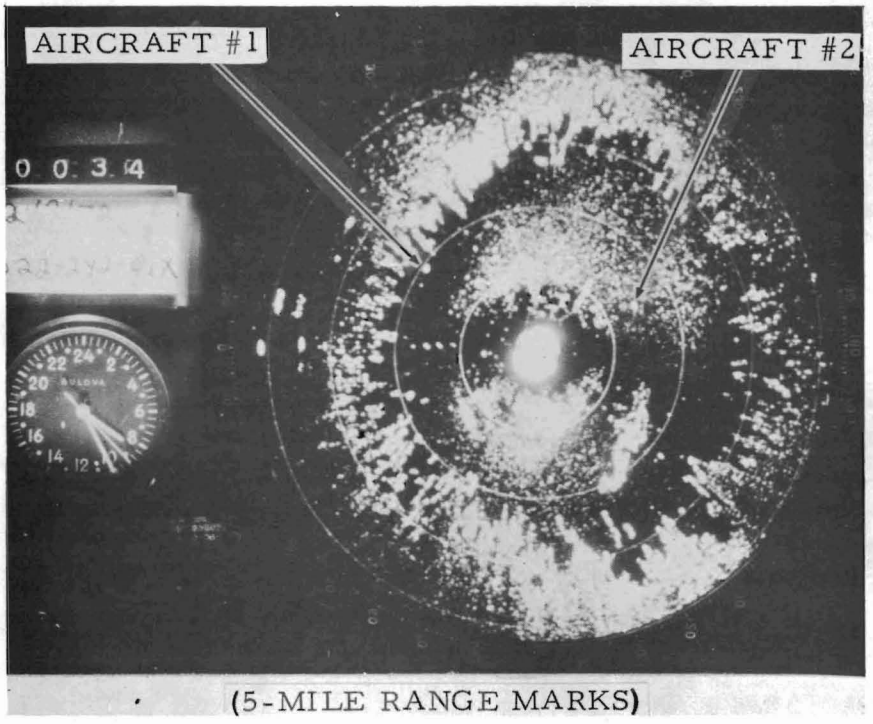

FIGURE 6. NONCOHERENT MTI TARGET DETECTION (5-MILE RANGE MARKS)

CIRCUIT DESCRIPTION. The frequency diversity circuitry consisted of a diplexer, video delay circuitry, normal and MTI video combiners, and a delay line oven temperature control circuit.

The diplexer was a three-port waveguide device providing 60-dB isolation between channel A (2710 MHz) and channel B (2795 MHz).

The delay circuitry consisted of video delay lines. One furnished a 1-μs delay to the ASR-5 channel B triggers so that the output of both transmitters would not be incident on the diplexer simultaneously. This in turn necessitated an equal delay in the channel A received video to make it coincident with that of channel B for application to the combiners.

The video combiners provided for additive and multiplicative combining of the channel A and B videos. Normal and MTI video combiners were provided. In the additive mode, the sum of the two videos was formed; in the multiplicative mode, the product.

The delay line oven temperature control circuit was provided to maintain the correct interchannel timing necessary for frequency diversity operation. The interpulse timing of channel B was slaved to that of channel A. Channel A and B trigger timing was compared to develop an error voltage which was used to regulate the temperature of the channel B delay lines in such a way as to maintain correct interchannel timing.

CIRCUIT TESTS. The video combiners and delay line oven temperature control circuits were investigated for correct operation.

Video Combiners. The video combiners were investigated to determine their target-processing characteristics by introducing test signals from S-band signal generators into the ASR-5 channel A and B directional couplers and plotting the output of the combiners as a function of the inputs. The signal from channel A was held constant while that of channel B was varied. The results for two values of channel A video in the additive and in the multiplicative modes are plotted in figure 7. These data show correct combiner operation.

Delay Line Oven Temperature Control Circuits. The delay line oven temperature control circuits were monitored for correct operation throughout the test period. Correct operation was determined by the maintenance of a 1-μs separation between channel A and B triggers. During this period, in the absence of ASR-5 synchronizer failures, correct timing was maintained. When ASR-5 synchronizer failures occurred, however, two problems became apparent. First, there was a thermal time lag following trigger interruption while the heat of the channel B ovens was regulated to bring the channels back in synchronism. In the worst possible case, when the channel B delay lines were cooled to ambient temperature, it took approximately 2 hours for stabilization at normal operation. Second, another problem resulted when the channel B trigger was lost. The oven control circuitry was set by the channel A trigger and reset by the channel B trigger with

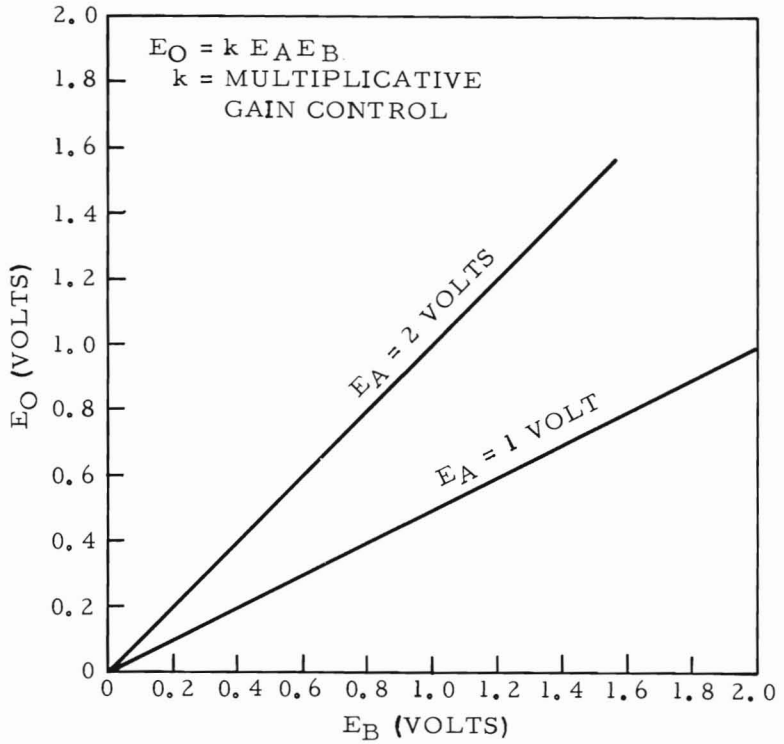

(a) MULTIPLICATIVE COMBINING

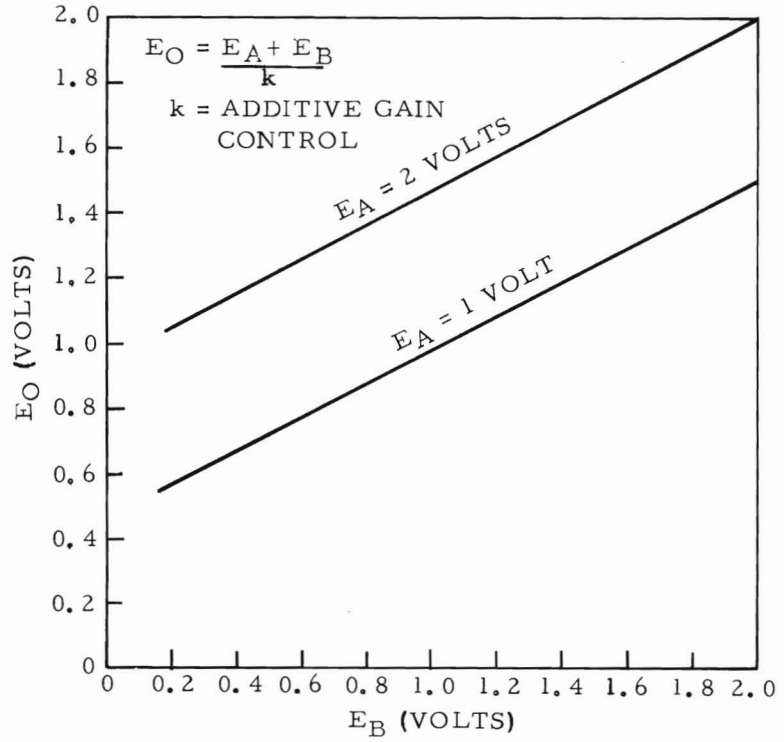

(b) ADDITIVE COMBINING

FIGURE 7. FREQUENCY DIVERSITY COMBINER PERFORMANCE

the time interval between controlling channel B delay line temperature. With no channel B trigger, the delay line overheated. Since the quartz delay lines had a negative temperature coefficient of delay, this resulted in the channel B trigger occurring before that of channel A. Once this condition was reached, the automatic temperature regulating circuit became inoperative, since reset occurred before set. To correct this problem, the channel B delay lines had to be cooled manually (by turning OFF the heater power). Also, the channel B trigger timing was sensitive to adjustments of the channel A and channel B cancellers. This was found to be due to the effect of the nonzero rise time of the system triggers on the modified trigger synchronization circuitry. Thus, when the cancellers were adjusted, channel B synchronism was lost. This made system alignment difficult.

TARGET PROBABILITY OF DETECTION. The loss of target video in the multiplicative mode when either channel's video output was low has been previously documented (reference 3), and it was presumed that only the additive mode was operationally acceptable. However, a limited amount of data were collected for both modes of operation in the absence of weather clutter to verify circuit operation.

MTI video from channel B was displayed on a PPI concurrently with delayed MTI video from the MTI video combiner. Photographs of the PPI display were obtained from each antenna scan, as shown in figure 8, to permit a comparison between single and dual channel operation. From this photographic data, an individual scan analysis and a blip/scan ratio were obtained for five aircraft trails; two of which were in the additive mode and the other three in the multiplicative mode.

For two aircraft trails in the additive mode (180 scans), the dual channel/single channel (B) blip/scan ratios were 1.0/.98 and .92/.58. The second trail, chosen deliberately, due to the noticeable degradation of channel B operation, indicated noticeable improvement was attained by dual channel operation. Channel B video never existed in the absence of dual channel video.

For the three aircraft trails (263 scans) obtained in the multiplicative mode of combining, dual channel video never existed in the absence of channel B video. Dual channel/single channel blip/scan ratios of .79/.985, .885/.97, and .72/.89 were obtained. These ratios confirmed that dual channel operation in the multiplicative mode degraded target probability of detection.

WEATHER REJECTION. An improvement in detecting targets in areas of weather clutter by the use of dual frequency diversity depends upon the decorrelation (between the two ASR-5 channels) of weather clutter video. Since the intent was to reduce the weather clutter without changing target signal strength, the combiners were adjusted to provide target video outputs equal in amplitude to the inputs. This resulted in reduced clutter signal levels due to the decorrelation discussed above.

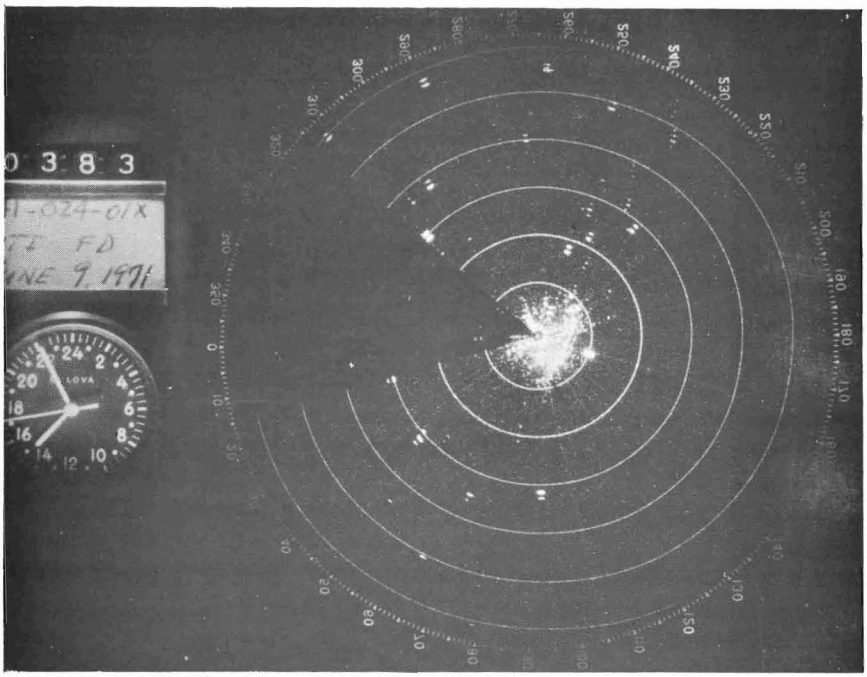

FIGURE 8. MTI MULTIPLICATIVE COMBINING PROBABILITY OF DETECTION

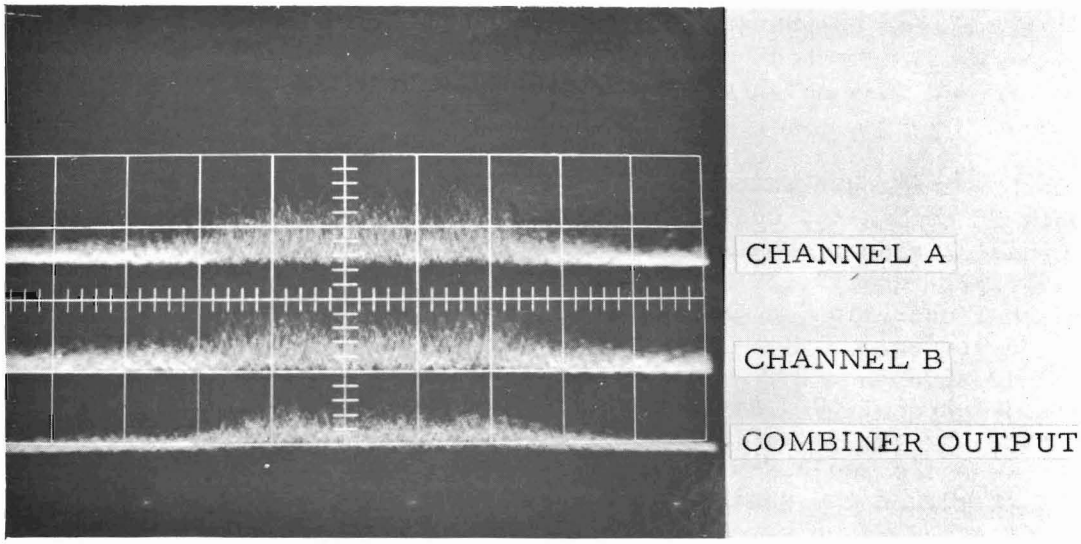

FIGURE 9. ADDITIVE COMBINING, WEATHER CLUTTER AND NOISE DECORRELATION

Additive combining clutter reduction is shown in figure 9. A 15-dB weather cell was spotlighted with the antenna and the two inputs and the output of the MTI combiner were displayed on a Tektronix 545A oscilloscope and photographed. Figure 9 shows that the output noise and weather clutter level was approximately half that of a single channel (a 6-dB reduction). For a large weather signal, such as shown in figure 10, the clutter reduction was somewhat less. To determine the amount of reduction, a variable attenuator was inserted in the ASR-5 channel B preamp MTI output. PPI photographs were then taken of the channel B MTI video display corresponding to various levels of attenuation. By comparing these photographs to photographs of the frequency diversity video display (no attenuation inserted), it was determined that between 3 and 6 dB of weather clutter rejection was obtained using additive combining.

In the multiplicative mode, greater weather-clutter rejection was realized. As seen in figure 7(a), a signal must be present from both radar channels for an output to be obtained. Therefore, due to the decorrelation capability of frequency diversity operation, the type of clutter rejection seen in figure 10 was obtained. The photographs show the PPI MTI presentation for single channel and multiplicative combined outputs. The weather clutter remaining after combining corresponded to areas of limit level clutter. Once limit level was reached, decorrelation was no longer possible. Since the combiners were placed in the system after the ASR-5 canceller video amplification and limiting circuitry, the limiter (normally set at approximately 15 dB above MDS) restricted the clutter rejection capability of the multiplicative combiner to 15 dB as shown in figure 10.

TARGET DETECTION. Target detection in weather clutter was determined by photographing the PPI presentation of aircraft target signals in weather clutter. An example of this is shown in figure 10, which shows the single channel MTI presentation, the corresponding MTI additive combiner presentation, and the corresponding MTI multiplicative combiner presentation. Additive combining provided an increased signal-to-clutter ratio over single channel operation. Note that the target signals in the clutter are more easily discerned. The amount of improvement corresponds to the weather clutter rejection capability discussed above. Multiplicative combining, by eliminating 15 dB of clutter, yielded greater subclutter visibility than additive combining. However, the lower probability of detection, discussed previously, also caused loss of targets.

LOGARITHMIC AMPLIFIER/FAST TIME CONSTANT (Log/FTC).

The theory of log/FTC operation is given in the literature (references 1 and 2). Basically, log/FTC action maintains receiver output noise levels constant and independent of the mean value of clutter signals. By thus reducing the dynamic range requirements of the PPI display, signals previously lost due to PPI saturation will now be visible. No improvement in signal-to-noise or signal-to-clutter is obtained.

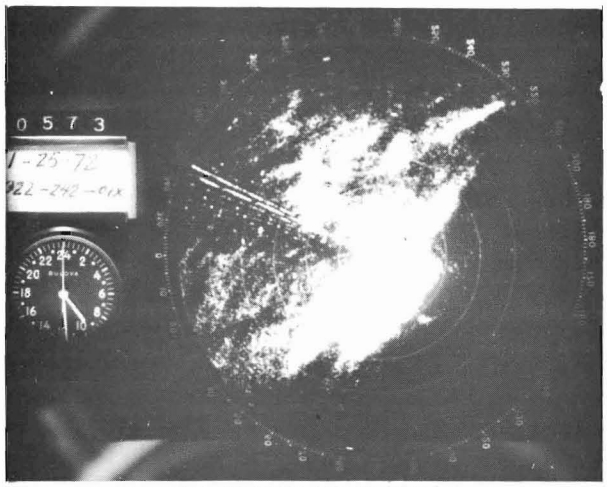

(a) SINGLE CHANNEL MTI VIDEO

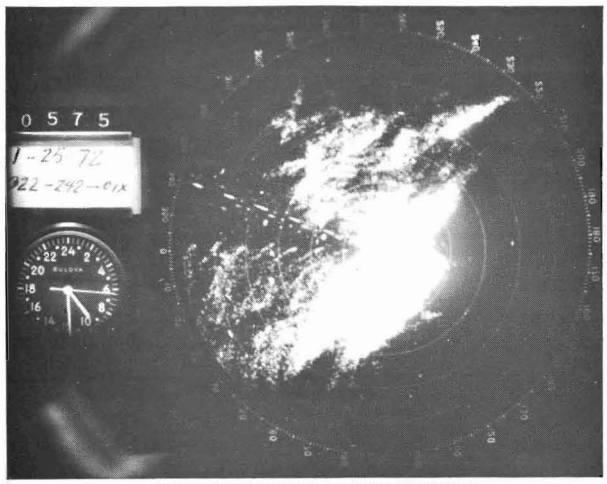

(b) ADDITIVELY COMBINED MTI VIDEO

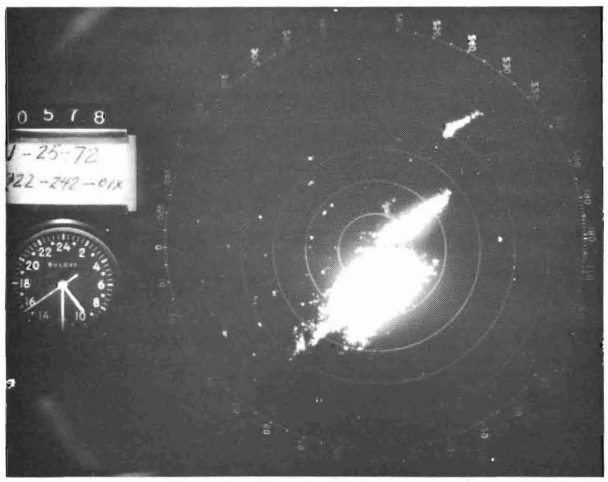

(c) MULTIPLICATIVELY COMBINED MTI VIDEO

FIGURE 10. FREQUENCY DIVERSITY CLUTTER REJECTION

CIRCUIT DESCRIPTION. The log/FTC equipment consisted of a video log amplifier, a fast time constant subtractor circuit, and an antilog circuit. A block diagram is shown in figure 11. Unipolar video (before amplification and limiting) from the ASR-5 cancellers was applied to a SN 55502 integrated log amplifier. The resulting log video was then applied to the fast time constant circuit which consisted of an integrator, delay line, and subtractor. In the integrator, consisting of a resistance capacitance circuit, signals of long duration (weather clutter) produced an output proportional to the mean value of the input. The delay line compensated for delays in the integrator. The subtractor then developed a signal that was the delayed input less the mean value of the input. Narrow signals (targets) passed relatively unchanged, while wide signals (weather clutter) had their mean value removed. The resulting video was then sent to the antilog circuit for restoration of the signal-to-noise ratio and then to the ASR-5 canceller chassis for amplification and limiting.

CIRCUIT TESTS. The log/FTC was tested for sensitivity, log response, antilog response, voltage stability, dynamic range, and overclutter visibility.

Sensitivity. Sensitivity was measured using standard MDS techniques. The input and output of the log/FTC circuits were monitored and compared simultaneously on a Tektronix 545A oscilloscope. It was determined that no loss of sensitivity was caused by the log/FTC circuitry.

Log/Antilog Response. Log response was determined by introducing the output of an S-band signal generator into the system and plotting the log amplifier transfer characteristic. The results are shown in figure 12. Logarithmic action was maintained throughout the allowable range of voltage inputs.

Antilog response was measured by using the same procedure as for the log response above to determine antilog circuit output as a function of log circuit input. The antilog output video test pulses were the same amplitude as at the log input indicating correct antilog action capability.

Voltage Stability. It was noted during the test period that operation of the log/FTC equipment was very sensitive to changes in the d.c. level at the input to the video log amplifier integrated circuit. Tests showed that a negative voltage shift resulted in a 1-dB loss in sensitivity for each 10 millivolts of shift, while a positive shift resulted in a corresponding increase in system noise levels. The circuitry was modified to provide greater voltage stability as discussed in appendix B. However, since the log circuitry was direct-coupled to the ASR-5 cancellers, small voltage levels generated in the canceller bipolar-to-unipolar converter circuits still resulted in significant changes in log circuit sensitivity. This problem was the limiting factor in correct log/FTC operation in extended areas of clutter as discussed later under clutter rejection.

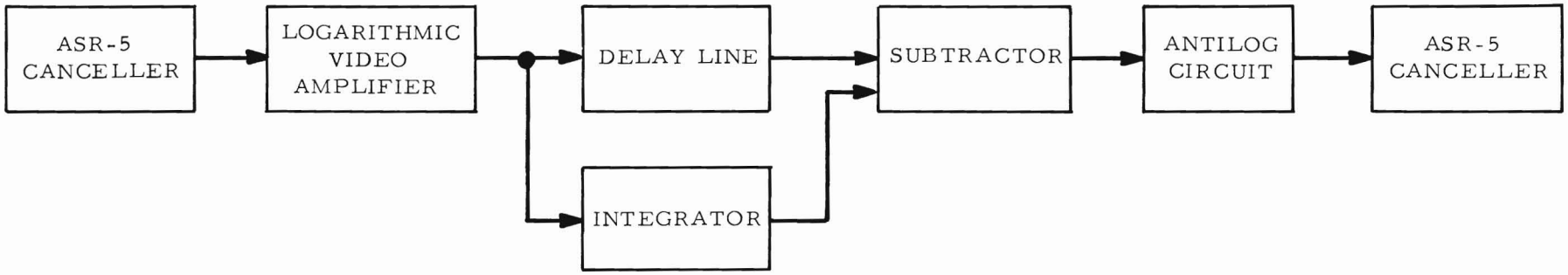

FIGURE 11. LOG/FTC CIRCUIT BLOCK DIAGRAM

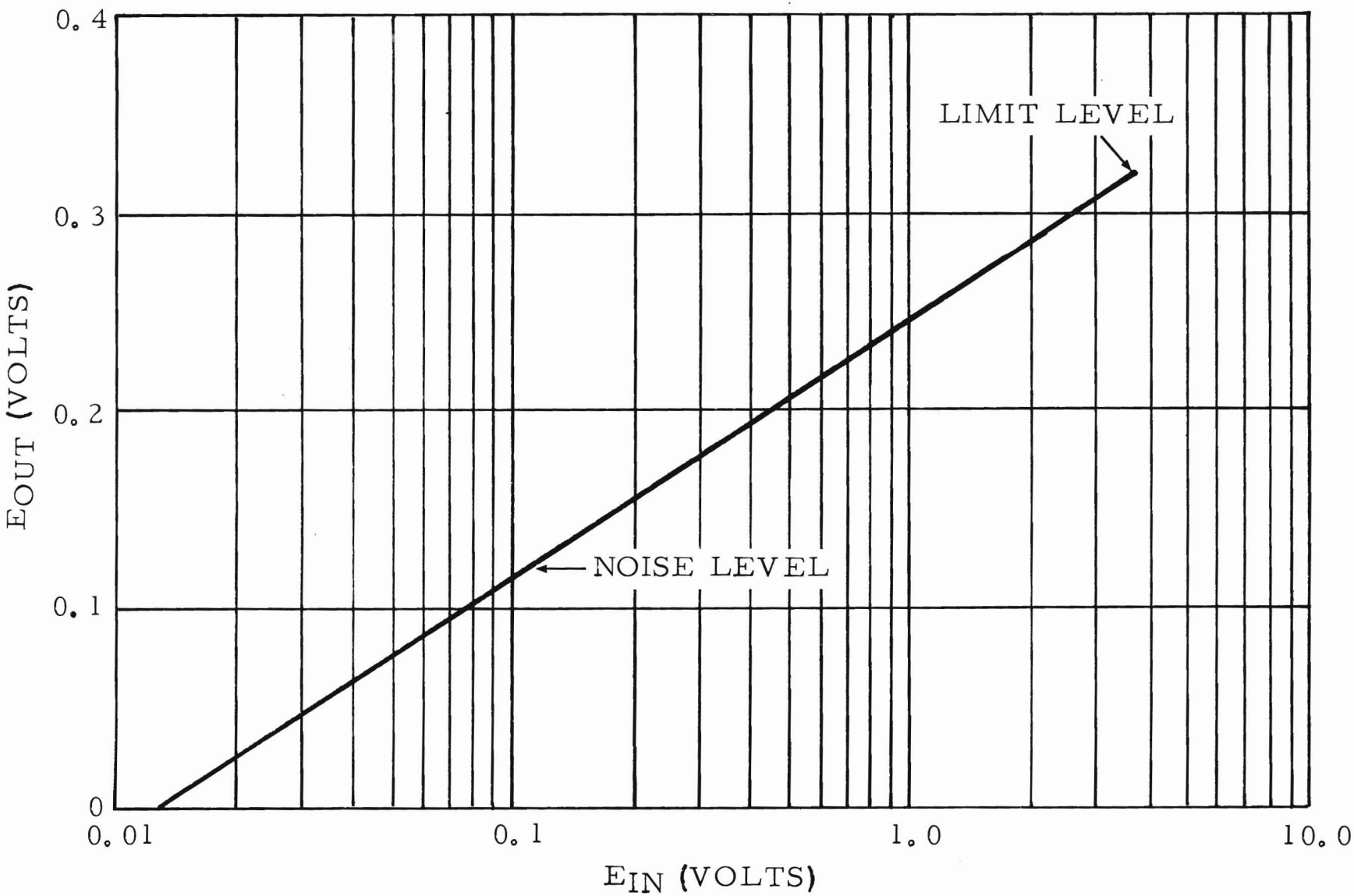

FIGURE 12. LOG AMPLIFIER TRANSFER CHARACTERISTIC

Dynamic Range. Dynamic range capability was determined by introducing an S-band test signal into an ASR-5 directional coupler and plotting the resulting video signal at the input to the video log amplifier as shown in figure 13. The maximum video amplitude obtained was thus determined to be within the dynamic range capabilities of the log integrated circuit as shown in figure 12. Figure 13 also depicts the dynamic range compression present in the ASR-5 MTI system. For the signal generator change of 38 dB, the video level changed by approximately 28 dB. The above dynamic range measurements were made with an ASR-5 MTI IF noise level, as measured at J6303, of 400 millivolts peak-to-peak. This value was arrived at by aligning the MTI system for noise equal to clutter residue as viewed on the system UPA-35 PPI.

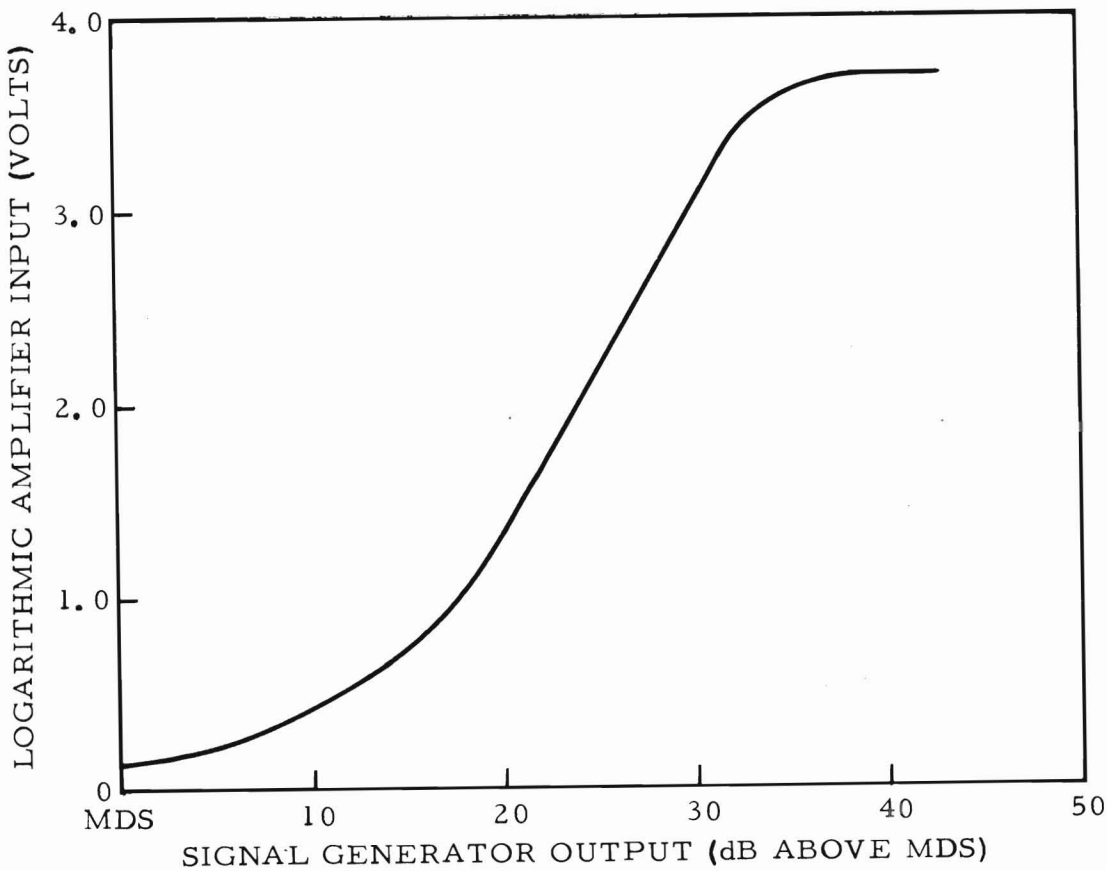

FIGURE 13. LOG AMPLIFIER INPUT VERSUS RF SIGNAL STRENGTH

Superclutter Visibilty. The superclutter visibility was determined using both a ring-around signal and an azimuth (simulated antenna scan effect) modulated signal superimposed on simulated clutter generated with a noise source. The ring-around and azimuth-modulated signals were both given radial velocities equal to that of an optimum speed target.

An MDS ring-around signal could be discerned on the PPI when no clutter was inserted. However, the azimuth-modulated signal became discernible at 6 dB above MDS with prior knowledge of its location and at 8 dB above MDS if its location was varied. This 8-dB difference was attributed to the integrating effect of the PPI phosphor and eyes with a ring-around signal.

When the signal level was set near the MTI system limit level (35 dB above MDS), and the clutter level was increased (figure 14), the ring-around signal was discernible until the clutter reached approximately 28 dB. Thus, the signal had to be 7 dB above the clutter to be discernible. The azimuth-modulated signal (35 dB and 240° as read on the photographically reversed compass rose) was discernible until the clutter level reached 20 dB (figure 15). The intensified area at 130°, as read on the compass rose, was caused by double exposure due to photographically overlapping a portion of two antenna scans. Thus, the azimuth-modulated signal level had to be 15 dB above the clutter to be discernible. The 8-dB difference in clutter level allowable for discerning a ring-around signal versus an azimuth-modulated signal corresponds to the 8-dB difference obtained when the clutter level was set to system noise level as discussed above. It should be noted that the target signal superclutter visibility obtained represented the maximum capability of the system, since the target signal was limit level and the simulated clutter was well behaved. As discussed later under target detection, this level of performance was not obtained with weather clutter.

CLUTTER REJECTION. Clutter rejection capability was determined using both simulated clutter from a noise source and weather clutter to determine the constant false-alarm rate (CFAR) action of the equipment.

The simulated clutter was introduced into the system, and the resulting output of the log/FTC circuitry was photographed on a PPI as the clutter level was increased. Figures 14 and 15 show the PPI presentation for several clutter levels. It can be seen that as the clutter level was increased, the residue on the PPI increased. This was due to the log/FTC circuitry not providing good CFAR action.

Figure 16 shows a weather cell 20 dB above MDS in maximum intensity and the same cell after log/FTC action. There was greater residue from the weather clutter than from simulated clutter signals of the same intensity. This was due to the nonuniformity of weather clutter in space, resulting in additional residue from the fast time constant subtractor circuit.

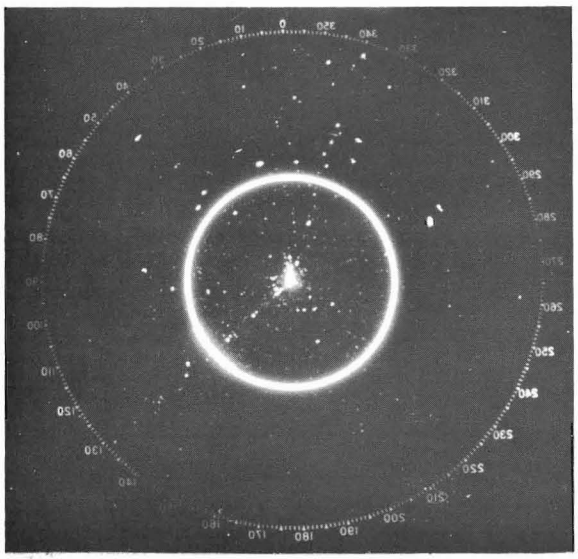

(a) 0 dB CLUTTER

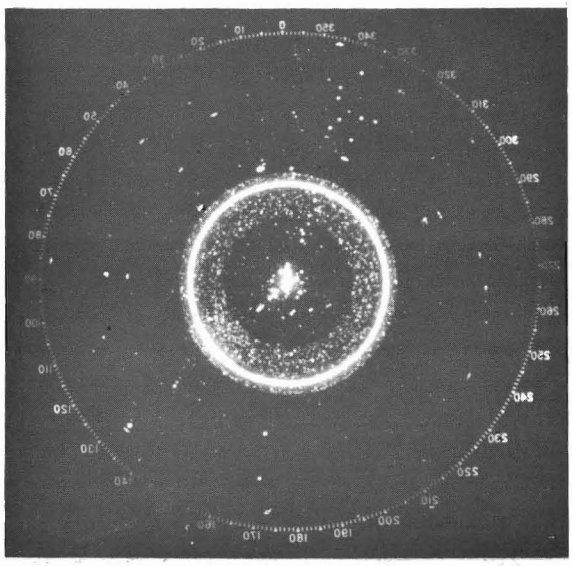

(b) 10 dB CLUTTER

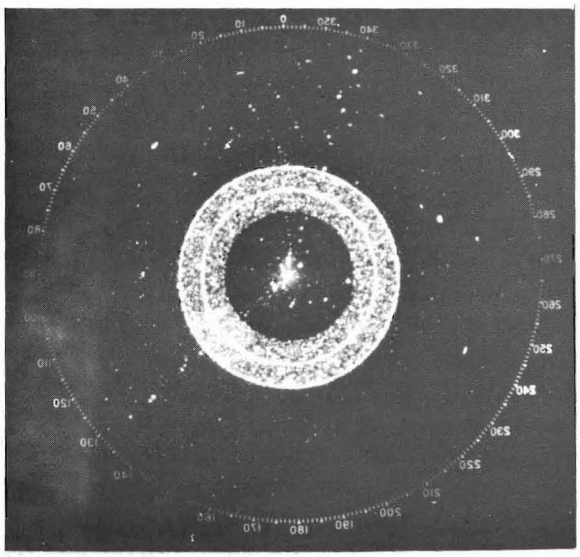

(c) 20 dB CLUTTER

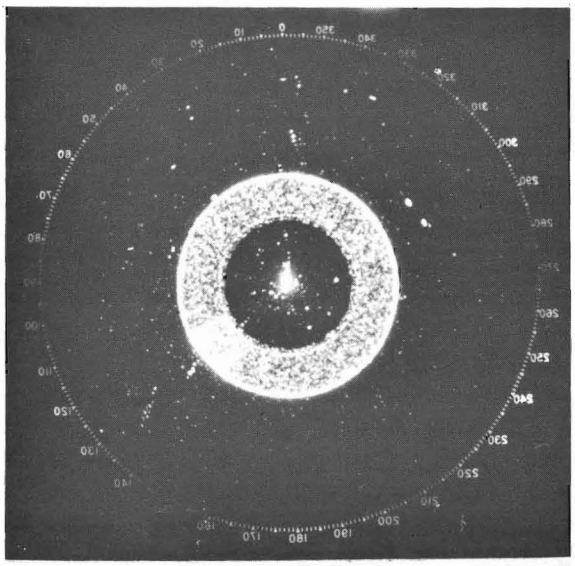

(d) 30 dB CLUTTER

FIGURE 14. LOG/FTC SUPERCLUTTER VISIBILITY OF A RING AROUND TARGET

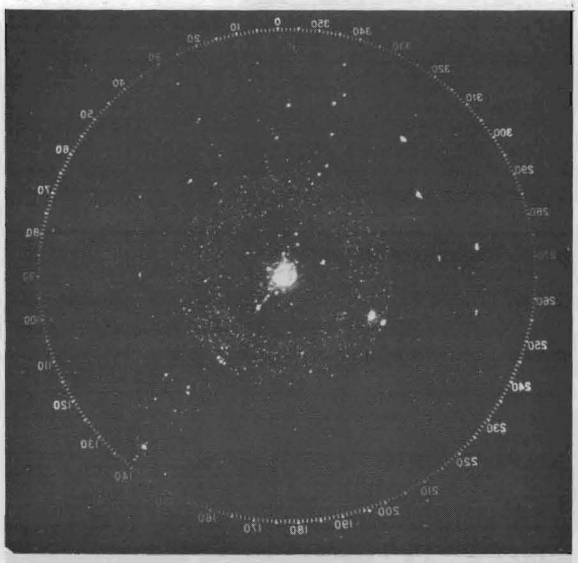

(a) 5 dB CLUTTER

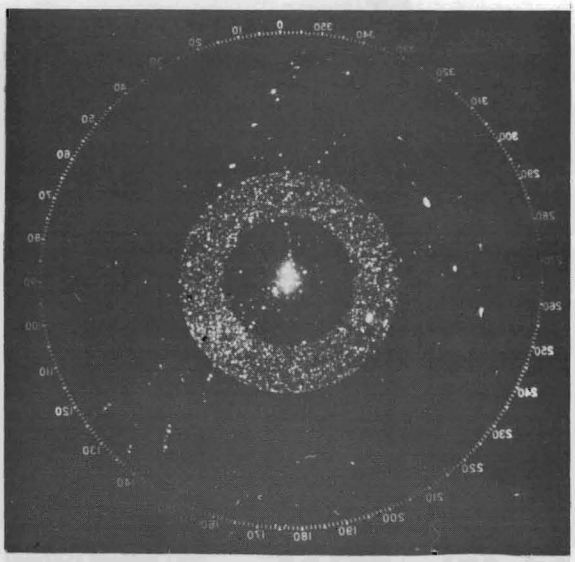

(b) 10 dB CLUTTER

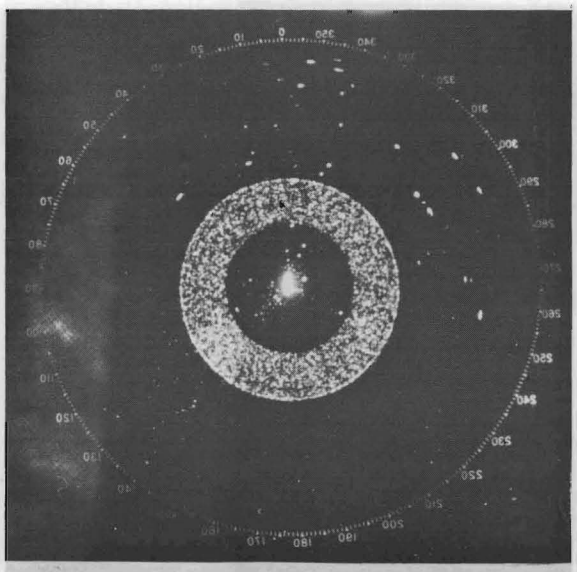

(c) 15 dB CLUTTER

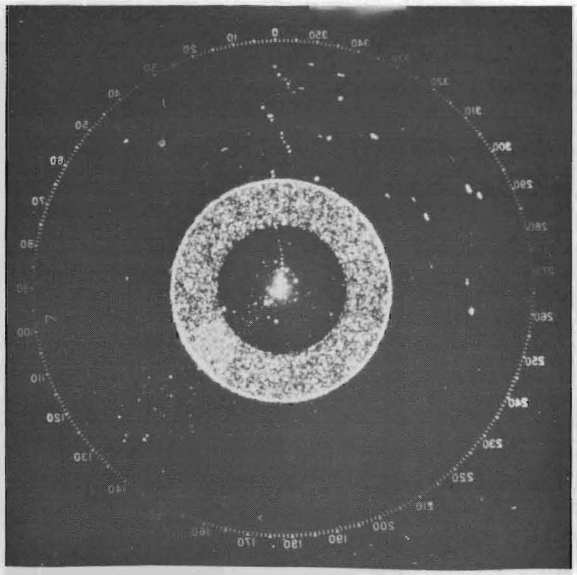

(d) 20 dB CLUTTER

FIGURE 15. LOG/FTC SUPERCLUTTER VISIBILITY OF AN AZIMUTH MODULATED TARGET

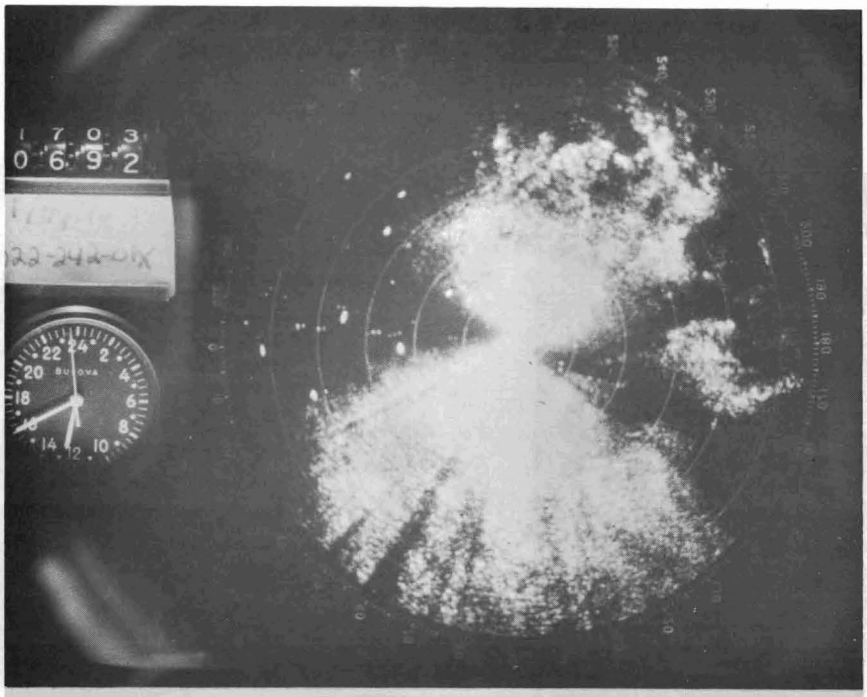

(a) MTI VIDEO

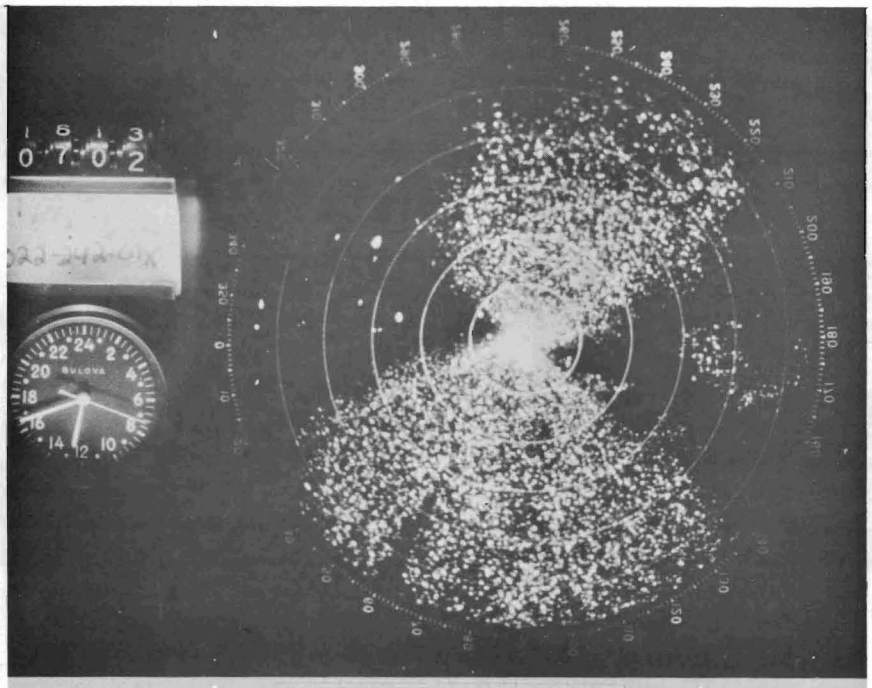

(b) LOG/FTC VIDEO

FIGURE 16. LOG/FTC RESIDUE

Figure 17 shows a weather cell with a maximum intensity of 30 dB above MDS. This large cell caused a greater positive voltage shift in the log input video baseline. As discussed above under voltage stability, this increased the circuit sensitivity resulting in increased noise and clutter residue levels as shown in figure 17. Note that blackholing occurred at the most intense portion of the weather, indicating that the log video amplifier was driven into limit.

TARGET DETECTION. Target detection capability was determined by tracking a limit-level-simulated target through areas of simulated clutter and weather clutter.

The results, using simulated clutter, are shown in figure 15. Note that the target at 240° became progressively weaker as the clutter level was increased. Target visibility was maintained until the clutter reached an intensity of 20 dB.

When using weather clutter, the maximum intensity clutter over which target detection was obtained was 15 dB. This 5-dB derogation in operation from that experienced using simulated clutter was caused by the greater residue experienced from operation of the log/FTC circuit on weather phenomena, as discussed above under clutter rejection.

Since actual target signals are generally of a lower level than the simulated targets discussed above, actual target detection capability would be less than that discussed above and would depend on the amplitude of the target versus that of the weather clutter. This was because no improvement in signal-to-noise or signal-to-clutter is obtained from log/FTC operation.

WEATHER CHANNEL.

For the detection and processing of precipitation clutter, a separate channel was incorporated into the ASR-5 system to provide for maximum weather clutter detection and weather clutter video formatting. The weather format consisted of two isoamplitude contours of weather intensity.

CIRCUIT DESCRIPTION. A simplified block diagram of the weather channel is shown in figure 18. The radiofrequency (RF) attenuator assembly utilized a PIN diode to provide both STC and gain control action on the received signals. ASR-7-type parametric amplifier, mixer, preamplifier, normal IF amplifier, and MTI IF amplifier and phase detector assemblies provided the video utilized in weather contouring. The video gate was used to select either MTI, normal, or range-gated MTI/normal video for contouring. The contour generator provided range integration, adjustable video-level thresholding, and selection of one or both isoamplitude contours for display. These contours were then mixed with the ASR-5 MTI video for display on the system PPI.

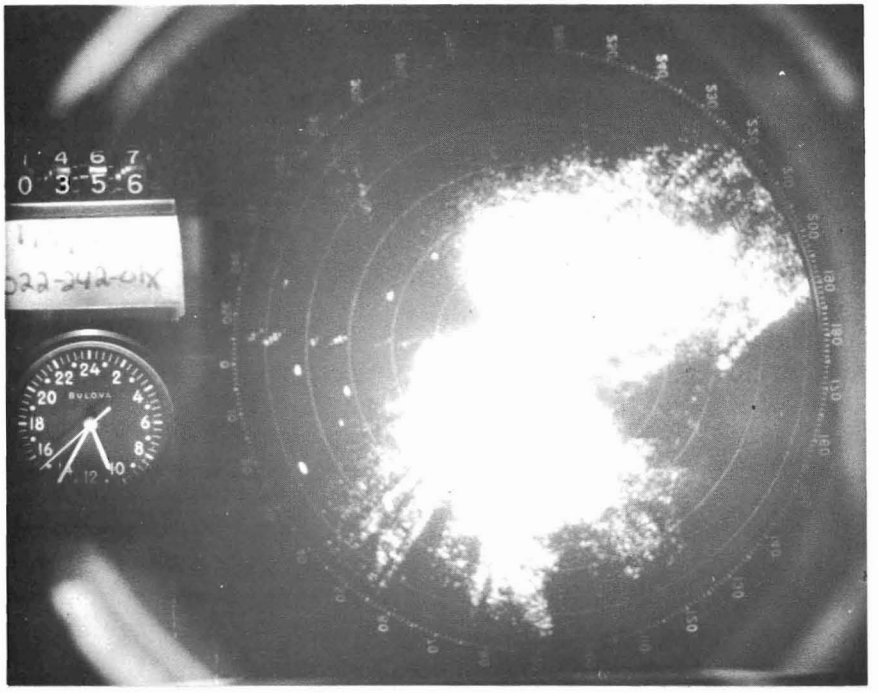

(a) MTI VIDEO

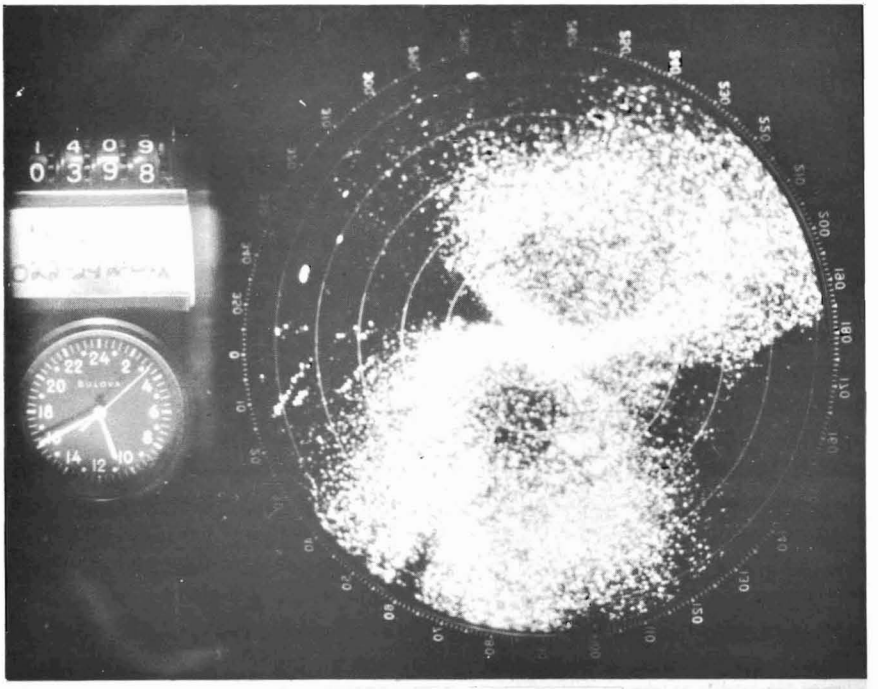

(b) LOG/FTC VIDEO

FIGURE 17. LOG/FTC RESIDUE AND BLACKHOLING

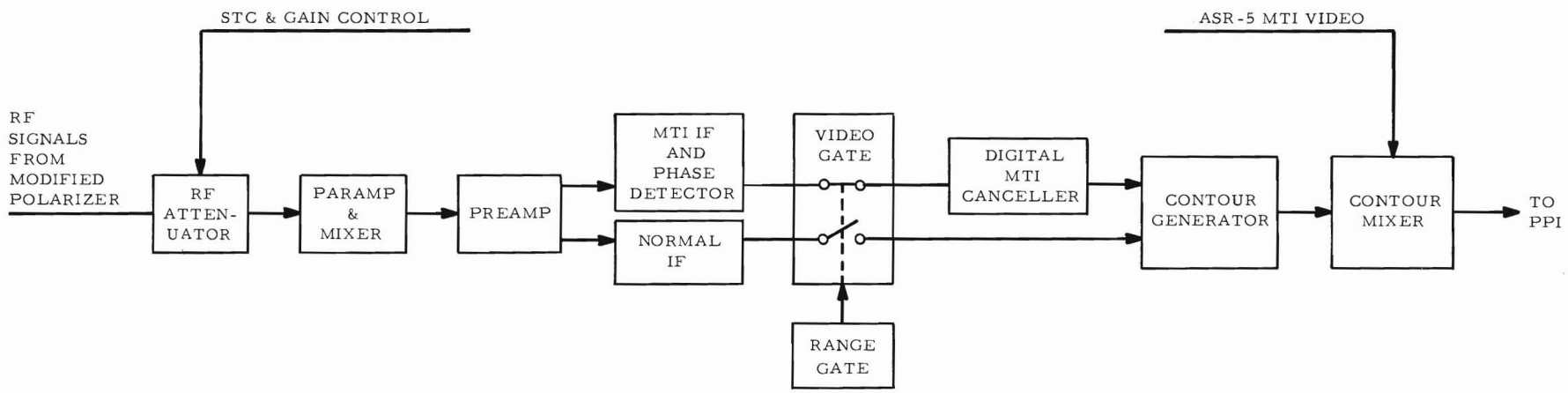

FIGURE 18. WEATHER CHANNEL SIMPLIFIED BLOCK DIAGRAM

CIRCUIT TESTS. The following portions of the weather channel were tested to determine their operational capabilities and characteristics:

Radiofrequency Attenuator. The RF attenuator was tested to determine its capability to provide selectable attenuation of received signals. An S-band signal generator output was introduced at the input to the RF attenuator through a coaxial directional coupler. The attenuation of this signal was then measured as a function of the gain control and sensitivity time control (STC) action.

The receiver gain control function was thus determined to be capable of providing the designed five preset attenuation levels.

The STC function was also thus determined to provide the desired attenuation of received energy as a function of range with the following exception. The maximum voltage level developed by the STC generator was 8 volts. Since the PIN diode assembly utilized in the RF attenuator provided an attenuation of 4 dB/volt, the maximum attenuation possible was 32 dB. The ASR-5 system at NAFEC used STC, cross-sectional sensitivity (CSS)-1, and CSS-2 curves of 35 dB, 50 dB, and 40 dB, respectively. Therefore, only the STC curve could be approximately matched with the attenuation capability provided.

Sensitivity. Sensitivity was determined by introducing an S-band signal generator output into the system as discussed above and using standard MDS techniques. The sensitivity of the normal receiver was determined to be -107 dBm and that of the MTI receiver to be -106 dBm.

Contour Generator. The contour generator was tested for its ability to generate accurate and well defined contours of weather signals. Figure 4 shows a weather signal and the corresponding contours. The intense portion of the weather (to the right of the photograph) yielded fairly well defined and accurate contours. However, the low-level scattered portions of the weather yielded random contouring which cluttered the display. From this and similar data, it was concluded that good contouring was provided when the weather clutter was in the form of intense well defined cells. However, when the clutter was low level and distributed, the contouring circuit produced excessive residue that made target detection difficult. Random contouring also produced unsatisfactory noncoherent MTI gating as discussed above under noncoherent MTI testing.

The video thresholding level portion of the contour generator circuitry furnished signals to both the contouring and noncoherent MTI clutter gating circuits. When the radar was in the circular polarization mode of operation, it was desirable to adjust the threshold level to provide clutter gating (for display of noncoherent MTI) to extend over areas of circular polarization punchthrough. At the same time, it was desirable to be able to adjust the threshold levels to provide contours corresponding to desired levels of weather intensity. Since the thresholding circuitry controlled both the contouring and clutter gating, these two functions could not be individually set as desired.

The contour generator was also tested for its ability to generate two isoamplitude contours of weather intensity. The two thresholding channels were identical and each was capable of generating contours as discussed above. However, due to the additional residue this would have introduced into the system, only one contour was utilized.

OVERALL SYSTEM TESTS.

Tests were performed to determine the compatibility of the four weather modifications and to determine their combined capabilities for clutter rejection and target detection. Photographic data were taken of the resulting video of the various possible combinations of modifications as viewed on the system PPI. These data were then analyzed to determine the resulting combined operation characteristics. During these tests, both ASR-5 transmitters were modified for narrow-pulse operation. Therefore, the combinations (all including narrow-pulse operation) which could be tested were:

1. Noncoherent MTI and log/FTC.

2. Noncoherent MTI and frequency diversity.

3. Log/FTC and frequency diversity.

4. All three modifications listed above.

Due to the probability of detection problem of the multiplicative frequency diversity operation, only the additive mode of MTI was utilized in these tests.

A modified STC curve, extending to 7 miles from the radar origin, was used to keep the ground clutter from limiting in the noncoherent MTI IF amplifiers.

WEATHER REJECTION. Figures 19 and 20 show a weather system and the clutter rejection achieved by combinations of the weather modifications. Each of the combinations is discussed below. Contours were displayed with the weather video. The weather had a maximum intensity of 35 dB above MDS.

Frequency Diversity and Log/FTC. Figure 19(d) shows residue similar to that experienced when using log/FTC by itself. This was to be expected, since the log/FTC circuits preceded the frequency diversity combiners in the system and had a greater effect in clutter reduction. The excessive residue shown was due to poor log/FTC CFAR action as discussed previously under log/FTC testing. Blackholing was again produced by the most intense portions of the weather, indicating that the log circuits were driven into saturation.

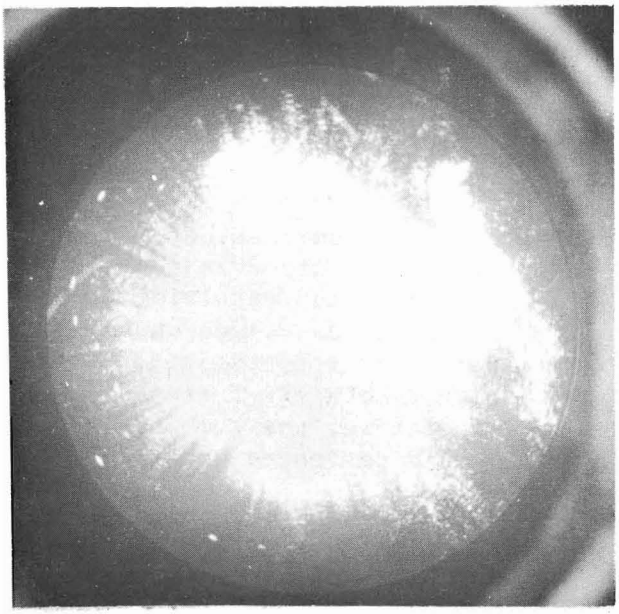

(a) NORMAL VIDEO

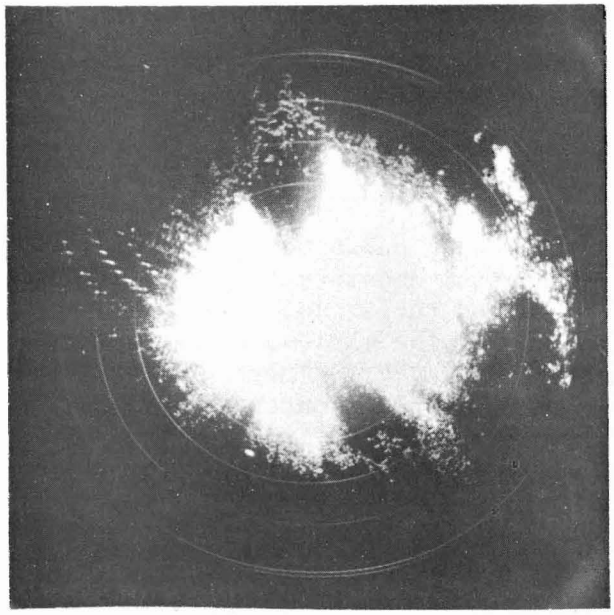

(b) FREQUENCY DIVERSITY

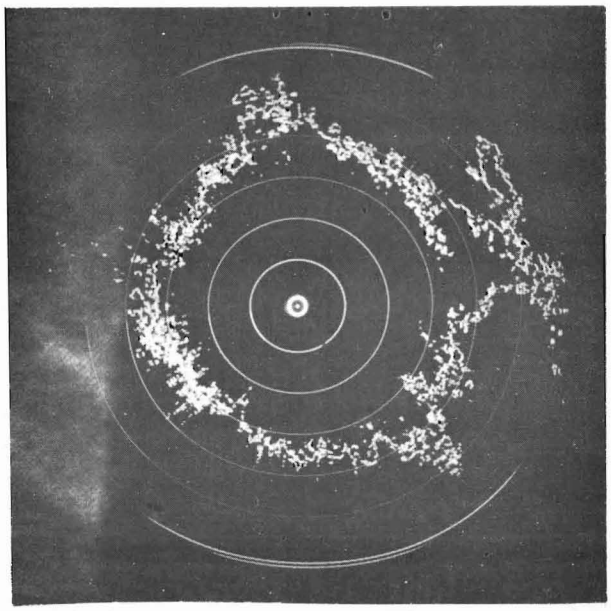

(c) CONTOURS

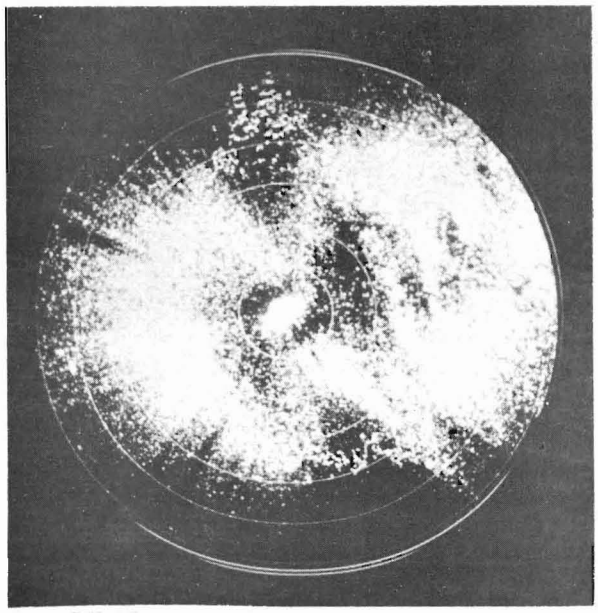

(d) FREQUENCY DIVERSITY AND LOG/FTC

FIGURE 19. SYSTEM WEATHER CLUTTER REJECTION (10-MILE RANGE MARKS AND 35-dB WEATHER)

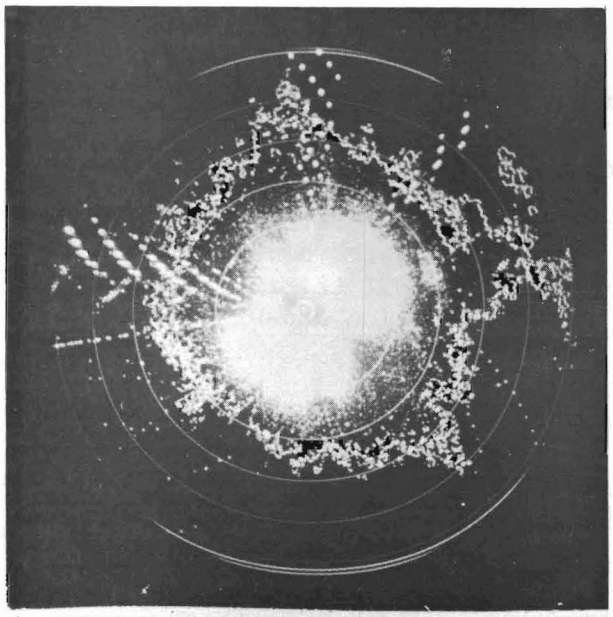

(a) FREQUENCY DIVERSITY AND NONCOHERENT MTI

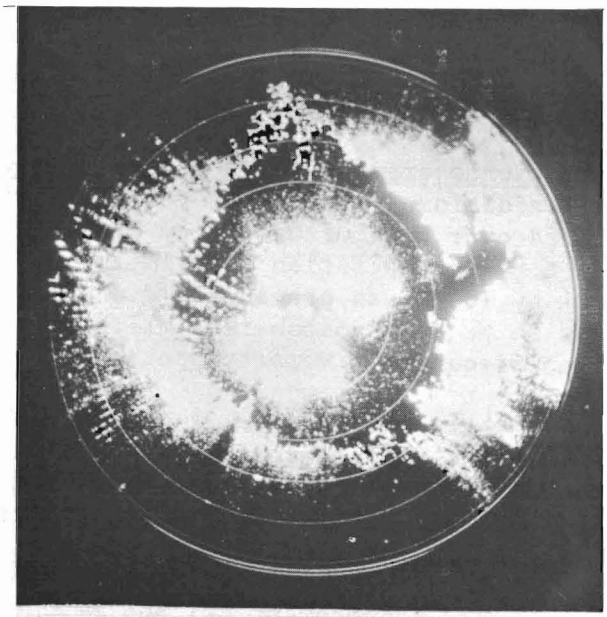

(b) FREQUENCY DIVERSITY AND GATED NONCOHERENT/ COHERENT MTI

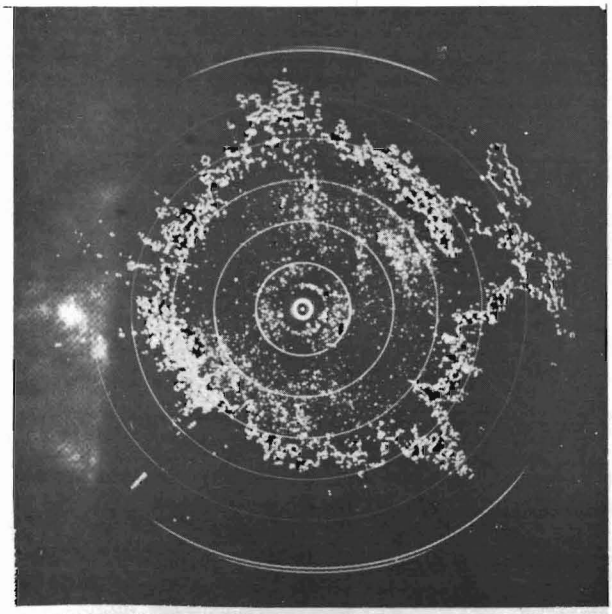

(c) FREQUENCY DIVERSITY, LOG/FTC AND NONCOHERENT MTI

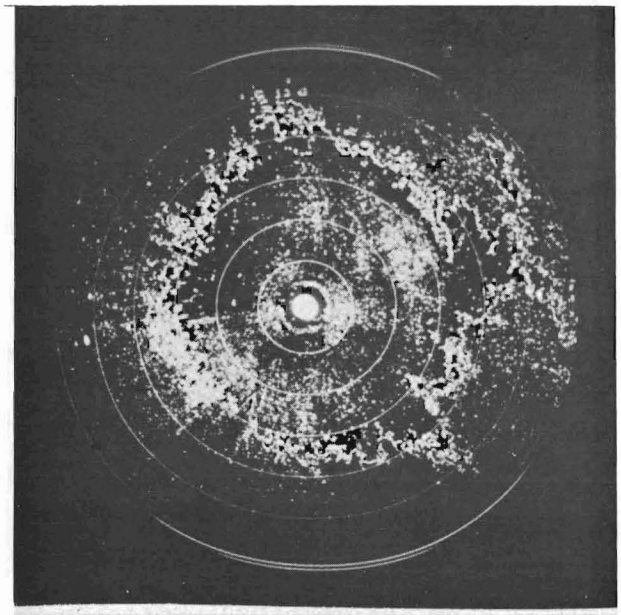

(d) FREQUENCY DIVERSITY, LOG/FTC AND GATED NONCOHERENT/ COHERENT MTI

FIGURE 20. SYSTEM WEATHER CLUTTER REJECTION (10-MILE RANGE MARKS AND 35-dB WEATHER)

An example of the combined effect of log/FTC and frequency diversity operation for a lower level (24 dB above MDS) and smaller in area weather signal is shown in figure 21. The addition of log/FTC to frequency diversity resulted in a lessening of the weather clutter. The CFAR problems of the log/FTC resulted in residue as shown. Some targets lost in the frequency diversity mode clutter became visible when using a combined operation.

Noncoherent MTI and Frequency Diversity. Figures 19(b) and 20(a) show the additional weather clutter reduction that noncoherent MTI (ungated) provided over that of frequency diversity alone. The weather clutter displayed in combined operation was similar to that obtained when using noncoherent MTI by itself as previously discussed under noncoherent MTI testing. This was so because noncoherent MTI had greater clutter rejection capabilities than frequency diversity operation.

Figure 22 (weather 22 dB above MDS) shows that frequency diversity complements noncoherent MTI operation. The weather residue shown for the combined operation was less than when using noncoherent MTI alone. Also, aircraft targets in the low-level portions of the weather were more easily discerned.

Gated noncoherent MTI and frequency diversity video is shown in figure 20(b). The additional clutter shown versus that of figure 20(a) was due to the effects of the clutter gating, as discussed under noncoherent MTI testing. As seen in figure 20(b), the areas of weather which were below the clutter gating threshold (and therefore outside the contours) were displayed as coherent MTI. This coherent MTI weather video was displayed as weather clutter on the PPI. Also, the clutter gating action contributed to the residue shown.

Log/FTC and Noncoherent MTI. As can be seen by comparing figures 20(b) and 20(d), the log/FTC circuitry was cabable of eliminating much of the residue associated with noncoherent MTI operation. Also, since the noncoherent MTI greatly reduced the intensity of the weather signals, the log/FTC was now better able to provide CFAR action.

The noncoherent MTI also complemented the log/FTC operation, as shown in figure 23. The weather shown was 15 dB above MDS in maximum intensity. The log/FTC circuit did not show the test signal in the weather for the reasons discussed previously under log/FTC testing. The noncoherent MTI, however, was able to display the test signal in the weather area. In combined operation (figure 23(d)), the test signal was displayed for 360°.

Noncoherent MTI, Log/FTC, and Frequency Diversity. Figures 20(c) and 20(d) show the combined operation of the weather modifications. In figure 20(c), the noncoherent MTI was operated in the ungated mode, eliminating gating and gated coherent MTI as sources of residue. In figure 20(d), the gated mode was used, resulting in increased residue. The weather shown was intense enough to cause limiting in the noncoherent MTI IF amplifiers. It was also of sufficient duration to cause saturation of the noncoherent MTI IF amplifiers. Therefore, the center portion of the PPI display does not give a good representation of system residue.

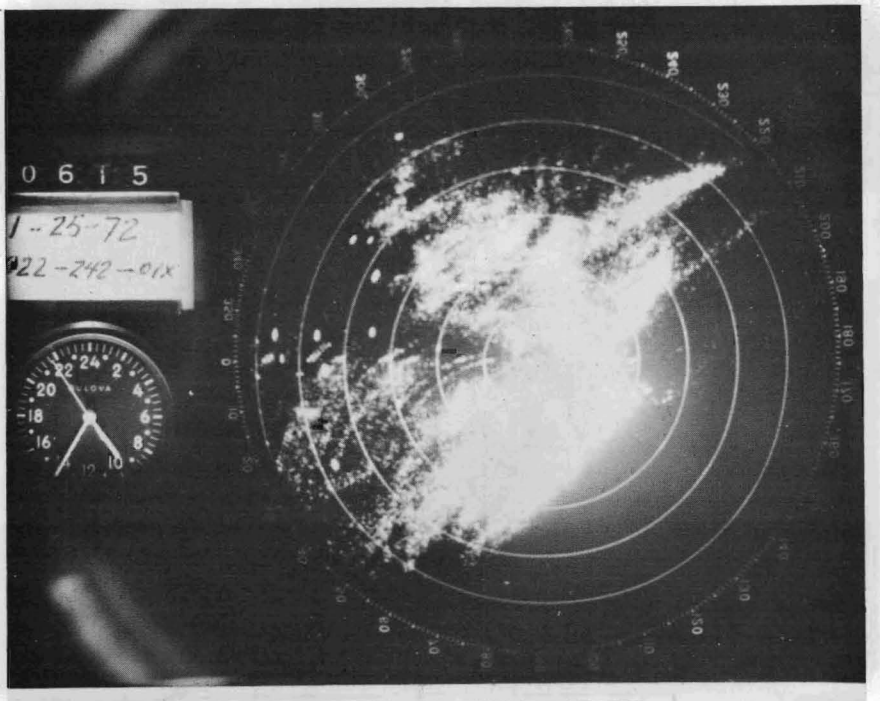

(a) FREQUENCY DIVERSITY

(b) FREQUENCY DIVERSITY AND LOG/FTC

FIGURE 21. COMBINED LOG/FTC AND FREQUENCY DIVERSITY WEATHER CLUTTER REJECTION (10-MILE RANGE MARKS)

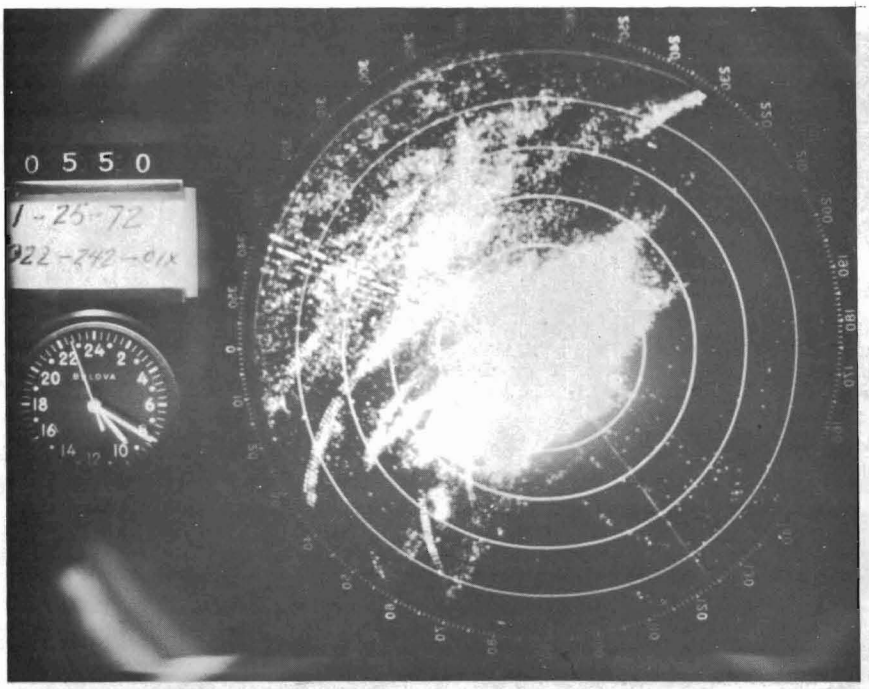

(a) NONCOHERENT MTI

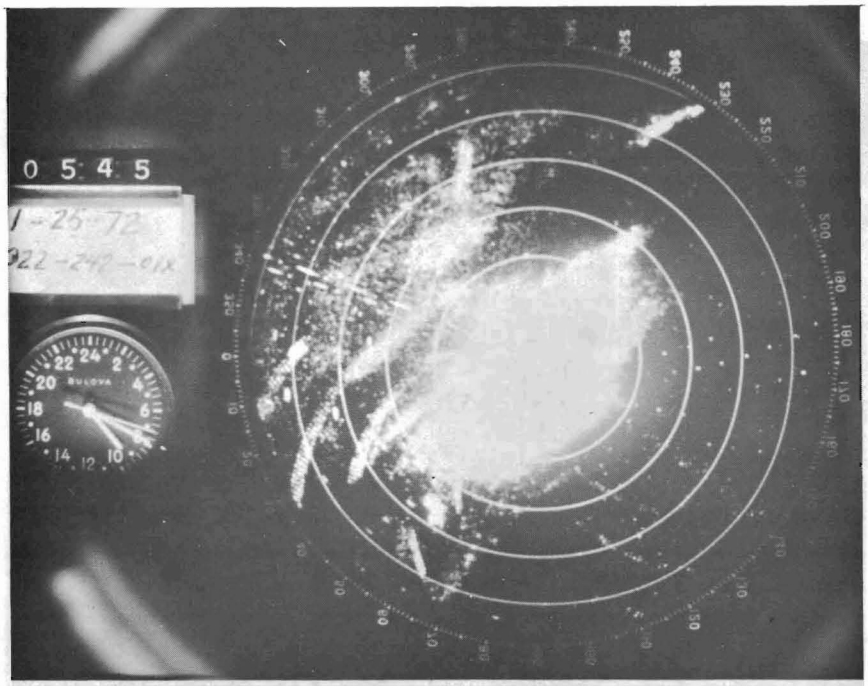

(b) NONCOHERENT MTI AND FREQUENCY DIVERSITY

FIGURE 22. COMBINED NONCOHERENT MTI AND FREQUENCY DIVERSITY WEATHER CLUTTER REJECTION (10-MILE RANGE MARKS)

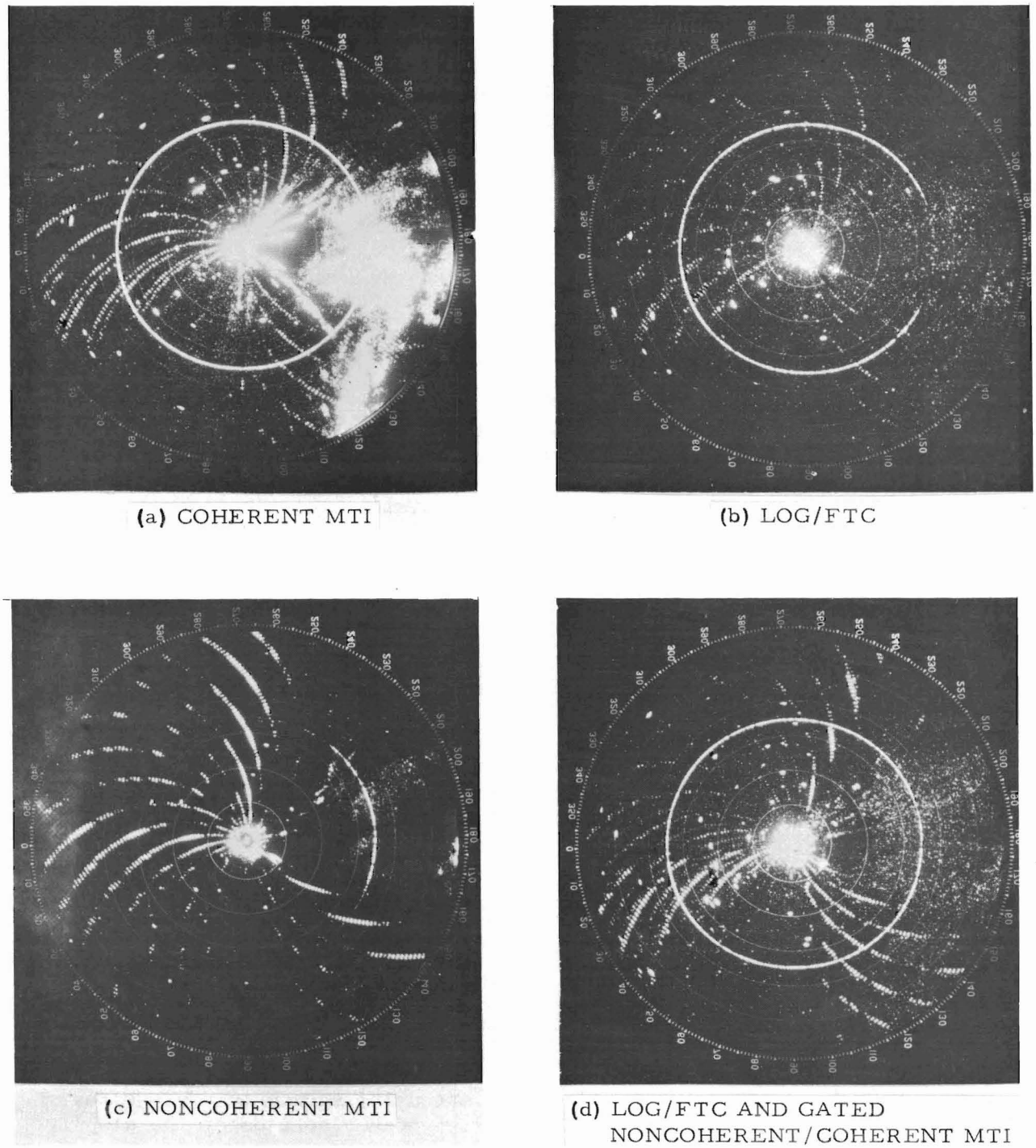

(a) COHERENT MTI

(b) LOG/FTC

(c) NONCOHERENT MTI

(d) LOG/FTC AND GATED NONCOHERENT/COHERENT MTI

FIGURE 23. COMBINED NONCOHERENT MTI AND LOG/FTC WEATHER CLUTTER REJECTION (10-MILE RANGE MARKS)

Figure 24 shows another weather system (30 dB above MDS in maximum intensity and smaller in area) along with the resulting display of the weather modification video. Note that in this figure more residue is shown in the center of the display. Due to the contour circuitry timing, the contours and the noncoherent MTI clutter gating began approximately 2 miles from the radar origin. Therefore, coherent MTI video was displayed within 2 miles resulting in increased weather clutter. The other residue near the PPI display center was due to the Doppler beat between the ground clutter and the moving weather clutter. This caused noncancellation of the resulting signal in the noncoherent MTI mode of operation. The residue at the periphery of the weather was caused by the noncoherent MTI gating and by the poor CFAR capability of the log/FTC.

In figure 25, another example is given of a weather system and the resulting residue. The weather system shown was 24 dB above MDS in maximum intensity. The residue shown was caused by the noncoherent MTI gating and by the poor log/FTC CFAR capability.

From these three examples, it can be seen that the degree of weather clutter reduction was dependent on the characteristics of each particular weather system. Also, in each case residue was generated by the operation of the weather modification, which partially obviated the desired effects provided. The effect of these limitations on system operation is discussed below under target detection.

TARGET DETECTION. Target detection capability was determined by photographing aircraft flying through areas of weather clutter as seen on the system PPI. These photographic data were then analyzed to determine system capability. For these tests, the system was operated with all the weather modifications. Target detection capability for four different types of weather is discussed below.

In the first example, the aircraft shown in figure 26(a) at 325° and 22 miles flew the inbound radial course depicted in figure 26(b). Note that the compass rose is shown in reverse. The target was not discernable while passing through the region of contour video and noncoherent MTI gating residue. It subsequently became visible at a range of 24 miles and remained so until it reached a range of 17 miles at which point it disappeared. Referring to figure 20(b), which represents the same weather system, it can be seen that the area of visibility corresponded to the dark annular region of noncoherent MTI between the noncoherent MTI weather video at the center of the display and the coherent MTI video and gating residue outside the contour area. The loss of the target when it entered the area corresponding to the noncoherent MTI weather video at the center of the display was caused by the limitations of the noncoherent MTI IF amplifiers. That is, the weather was near the IF amplifiers limit level and extensive enough to cause saturation of the IF amplifiers. Thus, although the center portion of the display was relatively free from residue, target detection was not possible.

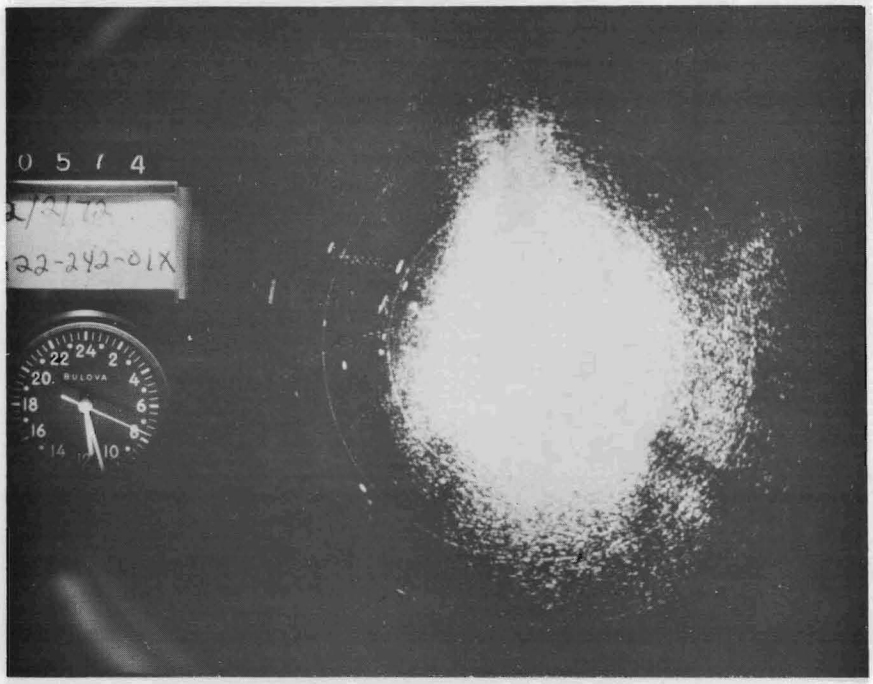

(a) NORMAL VIDEO

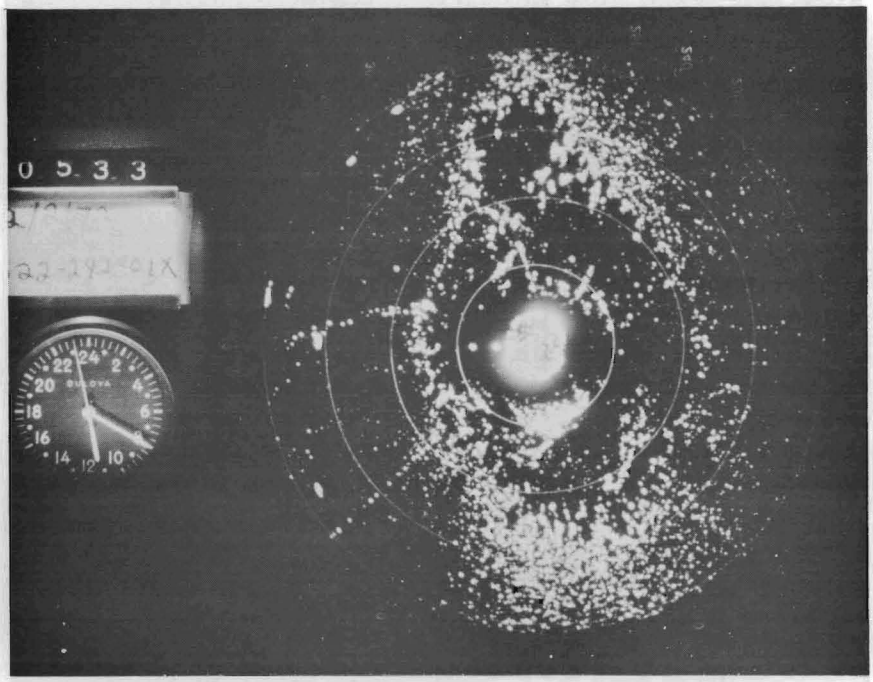

(b) WEATHER MODIFICATION VIDEO

FIGURE 24. SYSTEM WEATHER CLUTTER REJECTION (5-MILE RANGE MARKS AND 30-dB WEATHER)

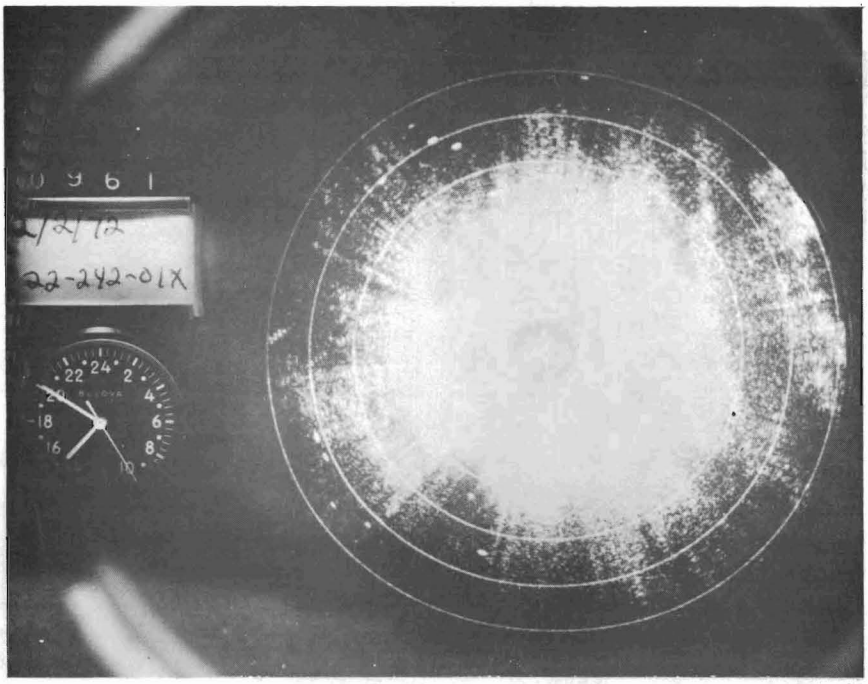

(a) NORMAL VIDEO

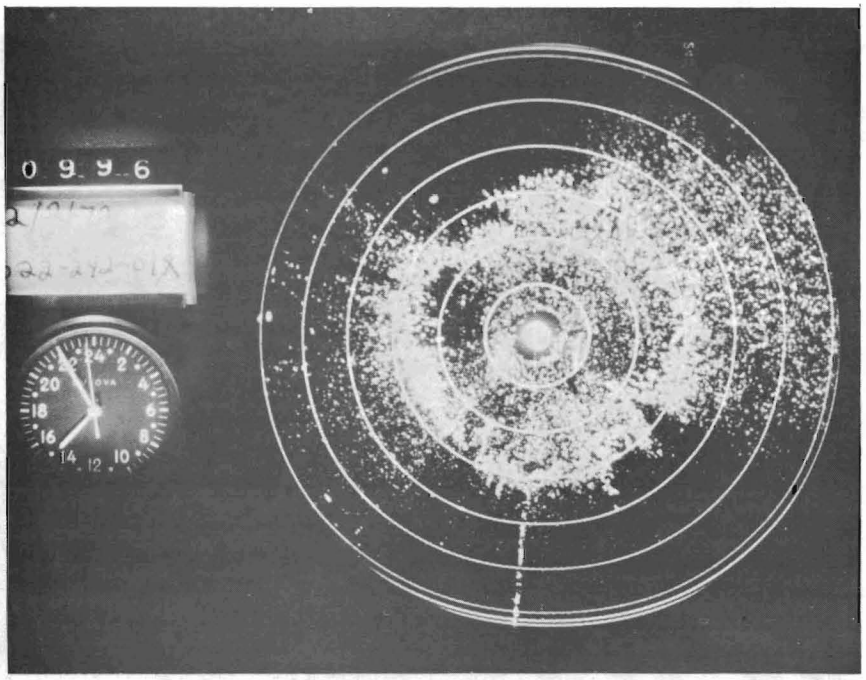

(b) WEATHER MODIFICATION VIDEO

FIGURE 25. SYSTEM WEATHER CLUTTER REJECTION (10-MILE RANGE MARKS AND 30-dB WEATHER

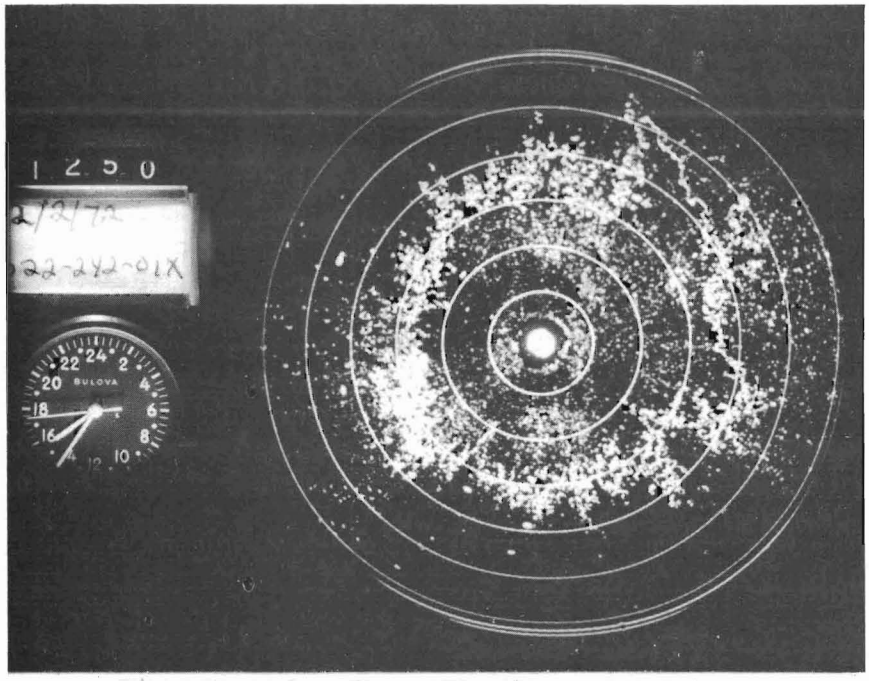

(a) WEATHER MODIFICATION VIDEO

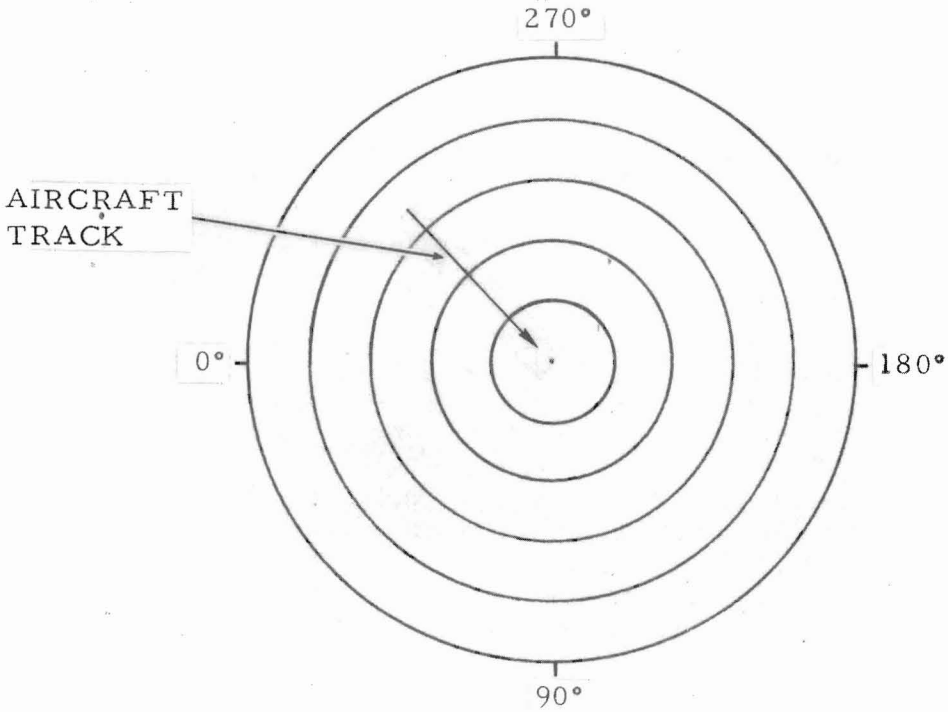

(b) TARGET TRACK

FIGURE 26. SYSTEM TARGET DETECTION (10-MILE RANGE MARKS AND 30-dB WEATHER

The second example of system target detection capability is shown in figure 24(b), representing a weather system which was smaller in area and had a lower maximum intensity (30 dB above MDS). In figure 24(b), an aircraft is shown at 340° and 8 miles in the noncoherent MTI gating residue. The PPI presentation azimuth reference is the same as given in figure 26(b). The aircraft was flying on an inbound radial course. Although the aircraft passed through an area of relatively little noncoherent MTI gating residue, it was lost for eight consecutive antenna scans. After passing through the residue region, it was subsequently visible until it reached the coherent MTI video residue at the center of the PPI display. Note that the aircraft would have been lost for a greater length of time on other radials proportional to the amount of residue on a particlar radial.

The third example (figure 25(a)) shows the target-detection capability for a weather system with a maximum intensity of 24 dB above MDS. An aircraft target is visible in the system residue at 64° and 18 miles. The PPI presentation azimuth reference is the same as given in figure 26(b). The aircraft was flying a radial inbound course. The target signal was lost in the area corresponding to the contour video and noncoherent MTI gating residue. The target then became visible at a range of 24 miles and remained so until it reached a range of 18 miles. The area of target visibility again corresponded to the area of noncoherent MTI lying between the noncoherent MTI weather video at the center of the PPI display and the noncoherent MTI gating residue. The target loss at 18 miles was caused by saturation of the noncoherent MTI IF amplifier and by residue generated due to the poor CFAR action of the log/FTC circuit.

The fourth example of system target detection is shown in figures 27, 28, and 29. For this test, the ASR-5 was operated with circular polarization. The video for the contours shown with the weather modification video was derived from the weather contouring channel. The weather clutter remaining in circular polarization operation is shown in figure 27(a) and had a maximum intensity of 15 dB above MDS. The tracks of two aircraft observed in this test are depicted in figure 29.

As shown in figure 27(b), the first track began at 265° and 34 miles with the target entering the clutter area. In figure 27(c), it had progressed to 260° and 25 miles and was barely visible in the noncoherent MTI gating residue. In figure 28(a), it is shown at 250° and 17 miles in an area free of residue. In figure 28(b), it was not detectable in the area of residue centered at 225° and 10 miles. This residue was due to the log/FTC not providing good CFAR action on a portion of the weather clutter which was not eliminated by the noncoherent MTI. In figure 28(c), the target is again shown at 170° and 12 miles between areas of residue.

The second aircraft being tracked was proceeding on an inbound course on the 8° radial as depicted in figure 29. The aircraft target is shown in figures 27(c), 28(a), 28(b), and 28(c) at ranges of 28, 21, 13, and 6 miles, respectively. The combination of noncoherent MTI gating residue, contour video, and residue due to poor log/FTC CFAR action cluttered the display in the track area and made target detection difficult as shown.

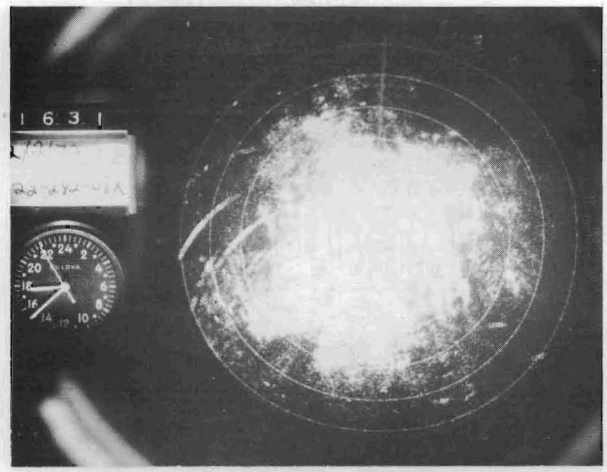

(a) NORMAL VIDEO

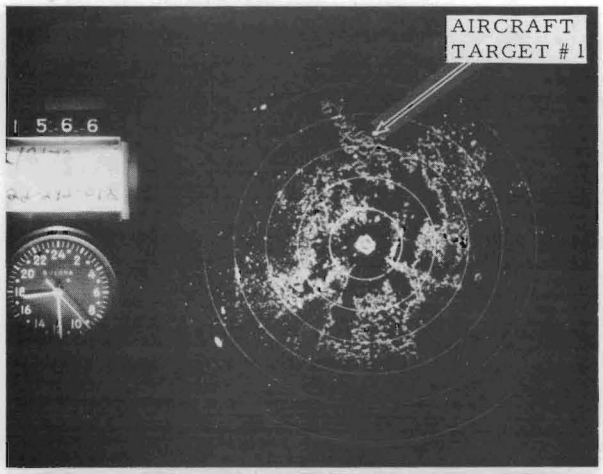

(b) TARGET AT 265 DEGREES AND 34 MILES

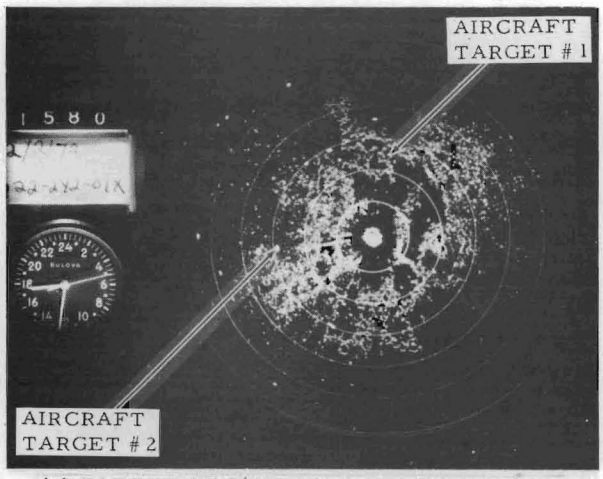

(c) TARGET AT 260 DEGREES AND 25 MILES

FIGURE 27. SYSTEM TARGET DETECTION (10-MILE RANGE MARKS AND 15-dB WEATHER)

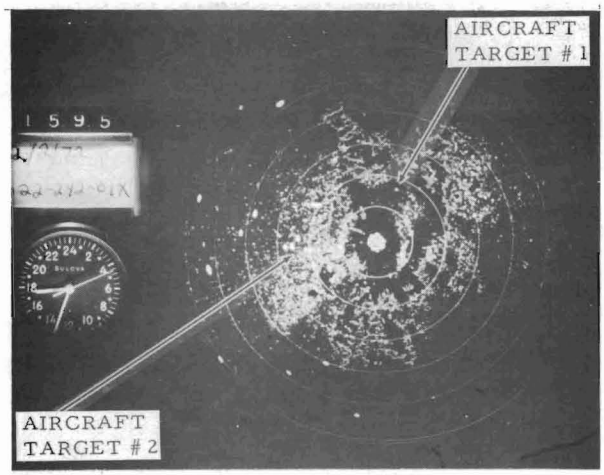

(a) TARGET AT 250 DEGREES AND 17 MILES

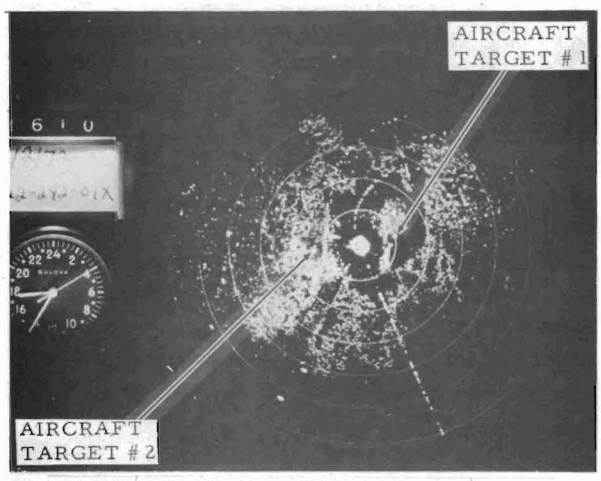

(b) TARGET IN CLUTTER AT 225 DEGREES AND 10 MILES

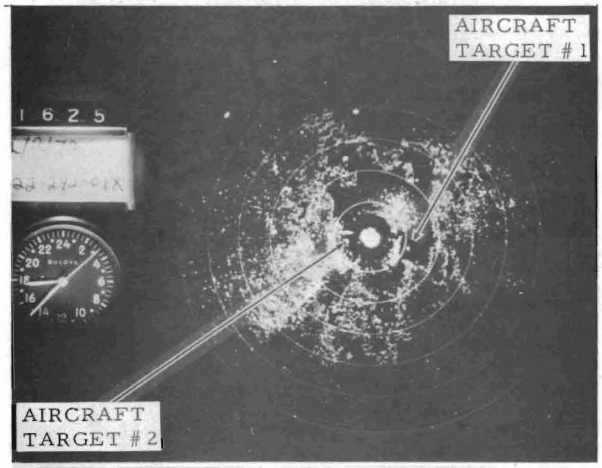

(c) TARGET AT 170 DEGREES AND 12 MILES

FIGURE 28. SYSTEM TARGET DETECTION (10-MILE RANGE MARKS AND 15-dB WEATHER)

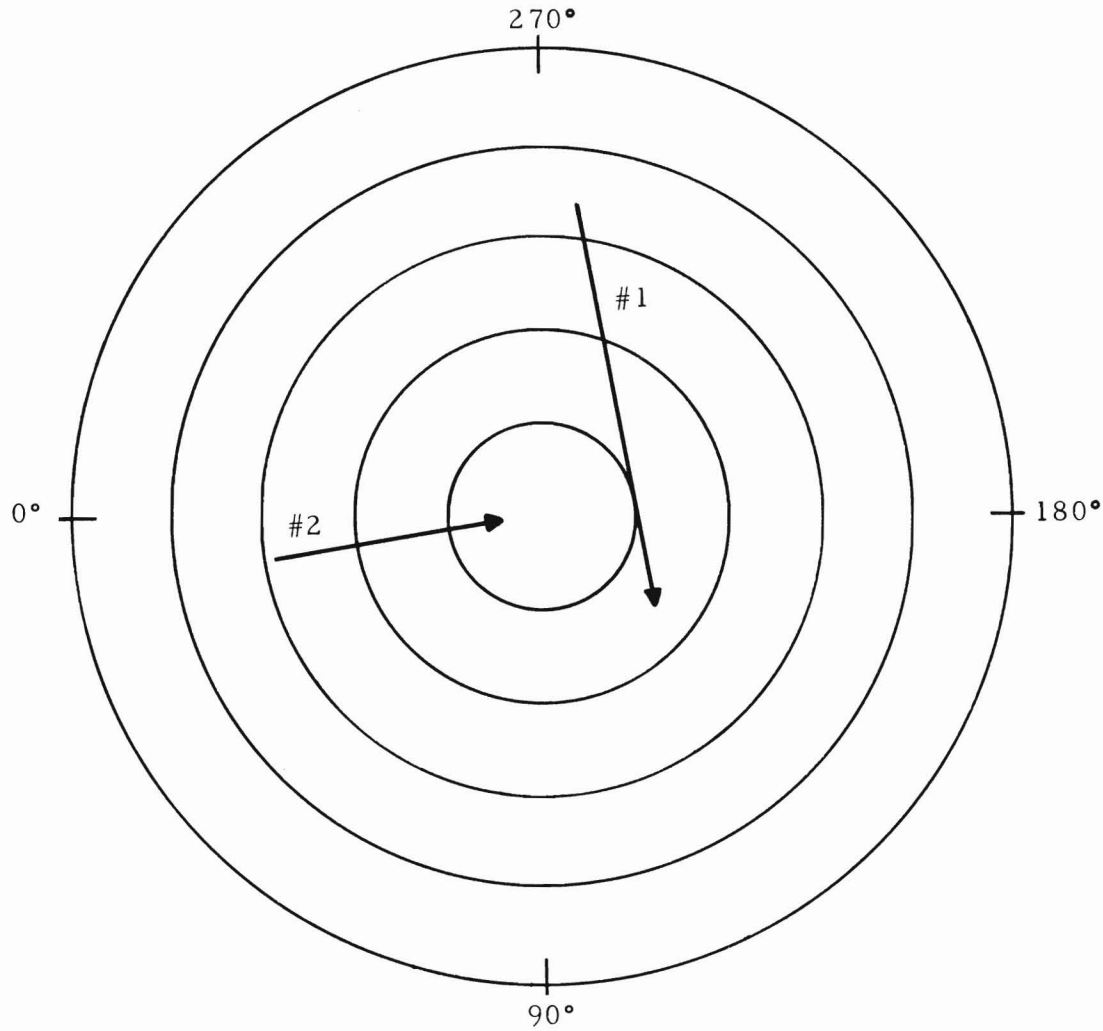

FIGURE 29. AIRCRAFT TRACKS

In summary, it can be seen from these examples that the system aircraft target-detection capability in weather was dependent on the nature of the weather clutter. Generally, target detection was not possible in the noncoherent MTI gating and contour video area. This was due to three factors:

1. Residue was generated by the noncoherent MTI clutter gate switching.

2. The contour video added to the PPI display clutter.

3. The log/FTC did not provide good CFAR action on the coherent MTI video in the gating/contour area.

In areas of higher intensity weather, target detection was limited by:

1. The limited dynamic range of the noncoherent MTI IF amplifiers.

2. The inability of the noncoherent MTI IF amplifiers to process large weather signals without saturating.

The inability of the log/FTC to provide good CFAR action on the non-coherent MTI weather video.

MODIFIED ASR-7 WEATHER TESTS.

Since the poor CFAR characteristics of the weather clutter feasibility model log/FTC circuitry did not permit a good evaluation of the noncoherent MTI log/FTC concept, an additional effort was made to do so. To this end, the NAFEC ASR-7 radar was modified to provide the desired videos. The block diagram of the modification is shown in figure 30. The ASR-7 MTI log/FTC circuitry provided the CFAR capability needed. Also, using this arrangement, a comparison could now be made with the weather clutter reduction and target detection capabilities of the ASR-7 normal/log receiver. Using this test configuration, either PPI could display normal log/FTC or noncoherent MTI log/FTC independently, or both videos could be displayed simultaneously. Simultaneous display of both videos was tried as an alternative to the dynamic clutter gating which previously resulted in gating residue.

Performance of the modified ASR-7 in a weather environment was tested using an RF test signal and a flight test aircraft. The test signal was used to evaluate the subclutter visibility performance, and flight testing was performed to determine aircraft detection in weather capabilities.

Figure 31 shows the relative test target detection capability in weather of noncoherent MTI, noncoherent MTI log/FTC, normal log/FTC, and the combination of the latter two videos. The weather shown was well behaved and below limit level, providing good noncoherent MTI operation. The test target was adjusted for an amplitude (10 dB above noise) well below the weather intensity level (28 dB above noise). These photographs show that noncoherent MTI can display targets not seen with normal log/FTC since normal log/FTC has no subclutter visibility in weather. It can also be seen that the combination of normal log/FTC superimposed on noncoherent MTI log/FTC provides somewhat better detection than either video by itself. However, the clutter residue and noise from both videos is also displayed.

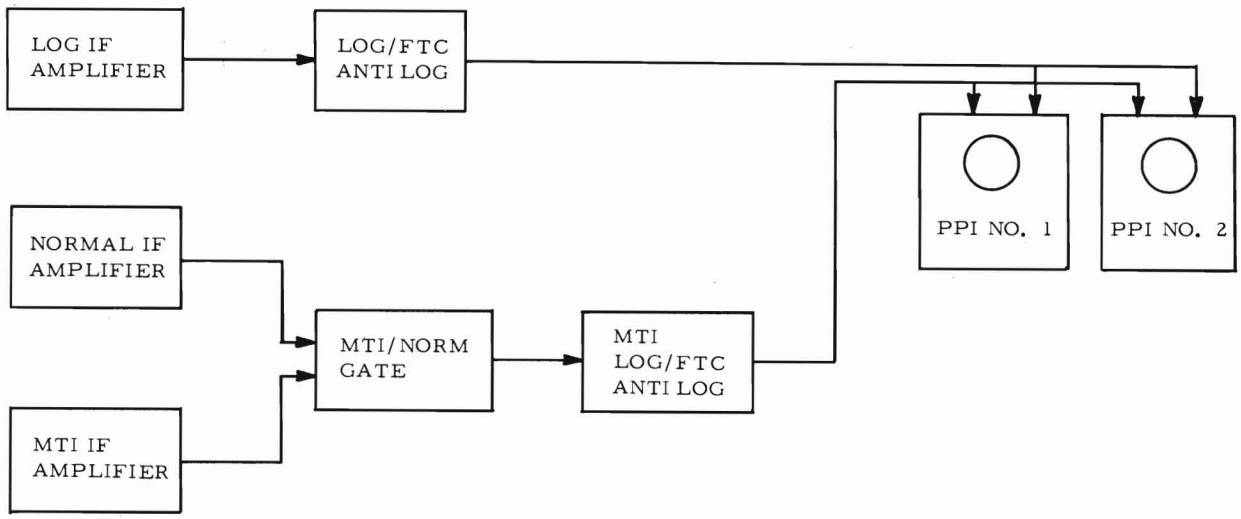

FIGURE 30. ASR-7 WEATHER MODIFICATION

As discussed previously, internal weather clutter motion results in noncancellation of the weather in noncoherent MTI processing. This residue, when it is subsequently applied to log/FTC circuitry, results in the degradation of target detection, since log/FTC provides no SCV capability. This is shown for the circuitry under test in figure 32. Figure 32 (b) shows the residue remaining after noncoherent MTI processing, and figure 32 (d) shows the inability of the subsequent log/FTC to extract the test signal from the residue background. Also, as shown, the low dynamic range of the ASR-7 normal receiver prevented noncoherent detection in high-amplitude weather signals.

Flight testing was conducted to determine the relative efficiency of the normal log/FTC and noncoherent MTI log/FTC receivers for target detection in weather. A Grumman Gulfstream (G-159) flight test aircraft was vectored through areas of weather clutter, and the resulting blip/scan ratios were calculated for both videos. For 151 scans of data, the blip/scan ratio for normal log/FTC video operation was 85 percent and for noncoherent MTI log/FTC, was 44 percent. The normal log/FTC video targets were also of much better quality.

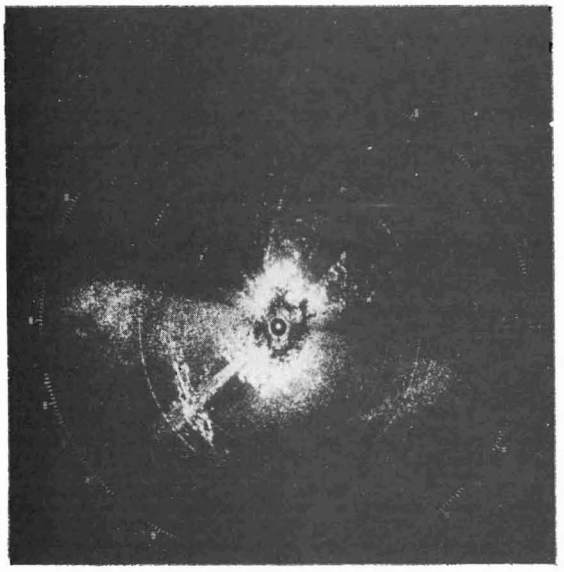

A. NONCOHERENT MTI

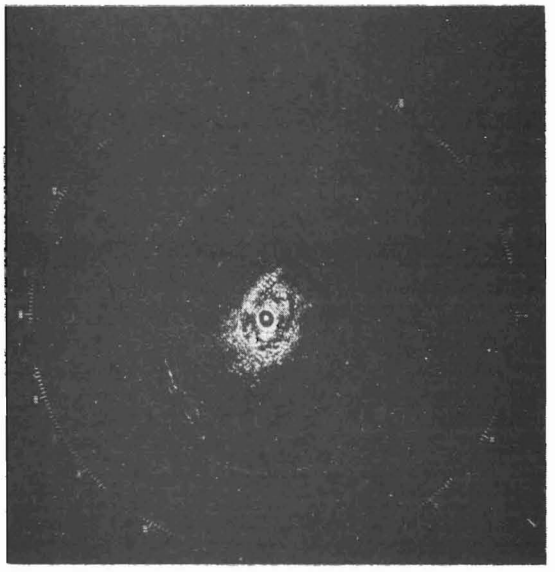

B. NONCOHERENT MTI
LOG/FTC

C. NORMAL LOG/FTC

D. NORMAL LOG/FTC AND
NONCOHERENT MTI
LOG/FTC

FIGURE 31. MODIFIED ASR-7 TEST TARGET DETECTION IN WEATHER

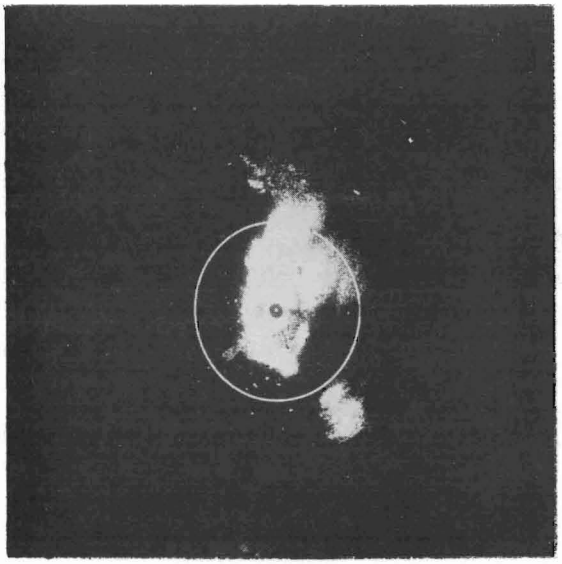

A. COHERENT MTI

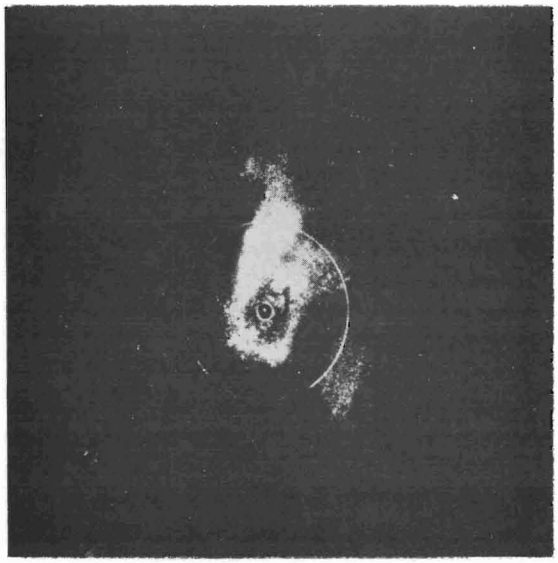

B. NONCOHERENT MTI

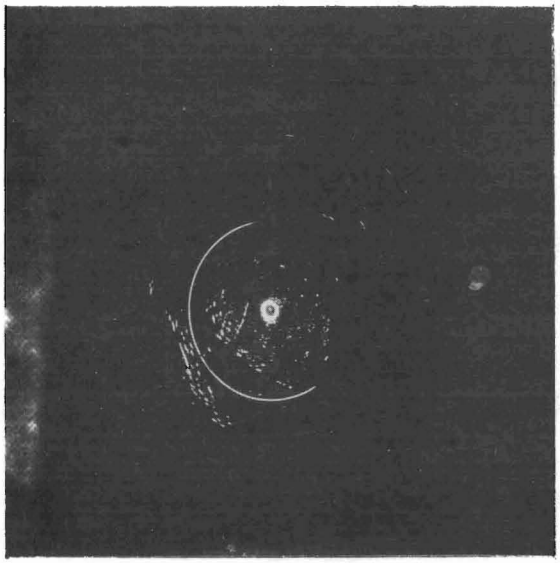

C. NORMAL LOG/FTC

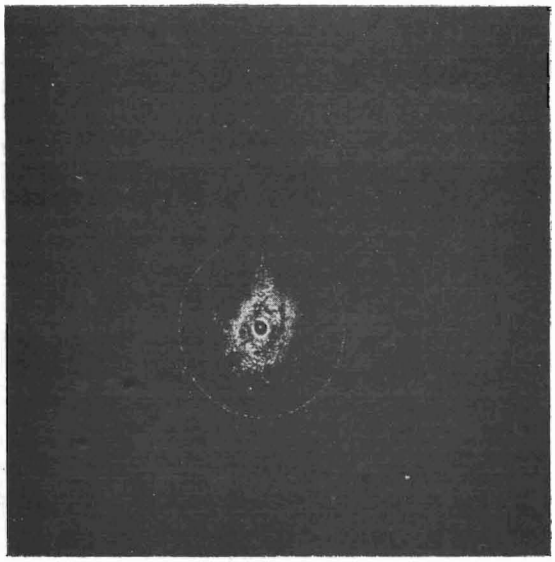

D. NONCOHERENT MTI
LOG/FTC

FIGURE 32. RELATIVE SUBCLUTTER VISIBILITIES OF MODIFIED ASR-7 VIDEOS

SUMMARY OF RESULTS

The results obtained during the evaluation of the weather clutter feasibility model are summarized as follows (results 1 through 18 apply to the contractor-furnished equipment; results 19 through 21 apply to the NAFEC-developed ASR-7 weather modification circuitry):

1. Target-detection tests produced blip/scan ratios of 71.3 percent and 70.4 percent for standard pulse width and narrow pulse width, respectively.

2. The theoretically predicted 3 dB of clutter rejection resulting from reduced pulse width operation was not verified, due to system instabilities and due to the decorrelation of weather signals with frequency diversity operation.

3. The noncoherent MTI provided up to 21 dB of subclutter visibility in weather. The amount of subclutter visibility obtained varied for different weather signals and was a function of the turbulence in the weather.

4. The noncoherent MTI IF amplifiers were saturated by large weather signals, resulting in loss of sensitivity.

5. The noncoherent MTI IF receivers had dynamic ranges of 35 dB.

6. The clutter gating for noncoherent/coherent MTI operation was good for well defined weather with steep gradients. It was poor for low-level scattered weather and resulted in cluttering of the system display.

7. The dual frequency diversity video combiners provided accurate additive and multiplicative outputs throughout their range of operation.

8. Additive frequency diversity combining resulted in up to 6 dB of weather clutter rejection.

9. Multiplicative frequency diversity combining resulted in up to 15 dB of weather clutter rejection. This was the maximum amount possible, since the combiners followed the ASR-5 MTI cancellers which had an output video limit setting of 15 dB.

10. Additive frequency diversity combining resulted in an increased probability of detection. Multiplicative combining resulted in a decreased probability of detection.

11. In the absence of ASR-5 synchronizer failures, correct frequency diversity interchannel timing was maintained. Synchronizer failures resulted in a decreased system reliability.

12. The log/FTC circuit did not provide CFAR capability.

13. With a limit-level-simulated target signal, the log/FTC provided over-clutter visibility in 20 dB of simulated (noise source) clutter and in 15 dB of weather clutter.

14. The weather channel normal and MTI sensitivities were -107 dBm and -106 dBm, respectively.

15. The weather channel contouring capability was good, for well defined high-level weather signals, and poor, for low-level scattered weather.

16. Independent threshold controls were not provided for the contours and the clutter gating circuits. This restricted the display of contours to weather clutter levels chosen for clutter gating and vice versa.

17. The combined weather modifications were capable of greater weather clutter rejection than was obtained from the individual modifications. The noncoherent MTI IF amplifier saturation and log/FTC CFAR problems distorted system operation so that the designed minimum 10 dB of clutter rejection was not uniformly obtained.

18. Target-detection capability in weather was a function of the characteristics of individual weather signals. The noncoherent MTI IF amplifier saturation, noncoherent/coherent MTI gating residue, and the poor CFAR capability of the log/FTC caused a loss of sensitivity and the generation of residue. This derogated target-detection capability.

19. Noncoherent MTI log/FTC operation utilizing the NAFEC ASR-7 system provided better operation than obtained from the similar portion of the weather clutter feasibility model. This was due to the better CFAR characteristics of the ASR-7 MTI log receiver. However, the amount of SCV improvement was still a function of the weather turbulence and intensity.

20. Using the modified ASR-7 system for a low-amplitude test target in well behaved, below-saturation weather, noncoherent MTI provided better test-target detection than either the coherent/MTI or log/normal receivers.

21. Modified ASR-7 aircraft target detection in weather tests produced blip/scan ratios of 85 percent and 44 percent for log normal/FTC and log noncoherent MTI log/FTC, respectively. Better quality targets were obtained with log normal/FTC operation.

CONCLUSIONS

Based on the results of the test and evaluation, it is concluded that:

1. The four weather modifications complement each other in weather clutter rejection. However, due to log/FTC and noncoherent MTI problems, the system does not satisfactorily provide the desired minimum of 10 dB of weather clutter rejection.

2. The weather channel does not provide acceptable contouring or contour-derived noncoherent MTI clutter gating capability.

3. The weather clutter feasibility model is not technically suitable for incorporation into existing ASR-5 radar facilities.

4. Due to the low dynamic range of the ASR-7 normal video circuitry and the turbulent characteristics of many weather systems, the ASR-7 as modified does not provide satisfactory combined noncoherent MTI log/FTC operation.

RECOMMENDATION

Based on the results of the test and evaluation, it is recommended that the weather clutter feasibility model not be considered for incorporation into FAA ASR systems.

REFERENCES

1. Skolnik, M. I., Radar Handbook, McGraw-Hill, 1970.

2. Nathanson, F. E., Radar Design Principles, McGraw-Hill, 1969.

3. Offi, D. L., Test and Evaluation Dual Diversity for Airport Surveillance Radars (ASR), System Research and Development Service, Atlantic City, New Jersey, Final Report No. RD-69-56, November 1969.

APPENDIX A

DESCRIPTION OF MODIFIED ASR-5

Figure A-1 shows the weather channel cabinet and basic subassemblies. Figure A-2 is a simplified block diagram of the ASR-5 weather modification. The following modifications and added assemblies comprised the weather modification.

TRANSMITTER MODIFICATION.

The transmitter was modified to operate at 800-kW peak-power output and with a .4-μs pulse width. To achieve this, the magnetron type was changed from a DX-276 to a JAN 5586, which was capable of handling the increased peak power. Also, the pulse-forming network was changed from two sections to one to match the pulse-forming networks rise time to that of the magnetron operated at a double peak power.

POLARIZER MODIFICATION.

The polarizer was modified by removing one of the loads from one arm of the polarizer and replacing it with a waveguide to coax transition. This modification permitted a portion of the circularly polarized energy received from spherical targets to be used in the weather receiver.

ROTARY JOINT.

The ASR-5 rotary joint was replaced with one having five channels. This provided the extra low-power S-band channel necessary for conducting the circularly polarized signal to the weather channel.

FREQUENCY DIVERSITY DIPLEXER.

A diplexer was installed in the waveguide system to enable operation in the frequency diversity mode. The diplexer consisted of two bandpass filters tuned to 2,710 MHz and 2,795 MHz. These two filters were connected through a "T" which provided the common output port. The diplexer provided a minimum of 60-dB isolation between input ports and an insertion loss of less than .5 dB at the desired frequency.

STABLE LOCAL OSCILLATOR (STALO).

The STALO energy for the weather channel was derived from the channel A STALO as shown in figure A-2. The cable (W2907), which normally connected the STALO to the automatic frequency control mixer, was replaced with a low-loss cable. The additional power made available was then, by use of a power divider, used to drive both the automatic frequency control mixer and the contour channel mixer.

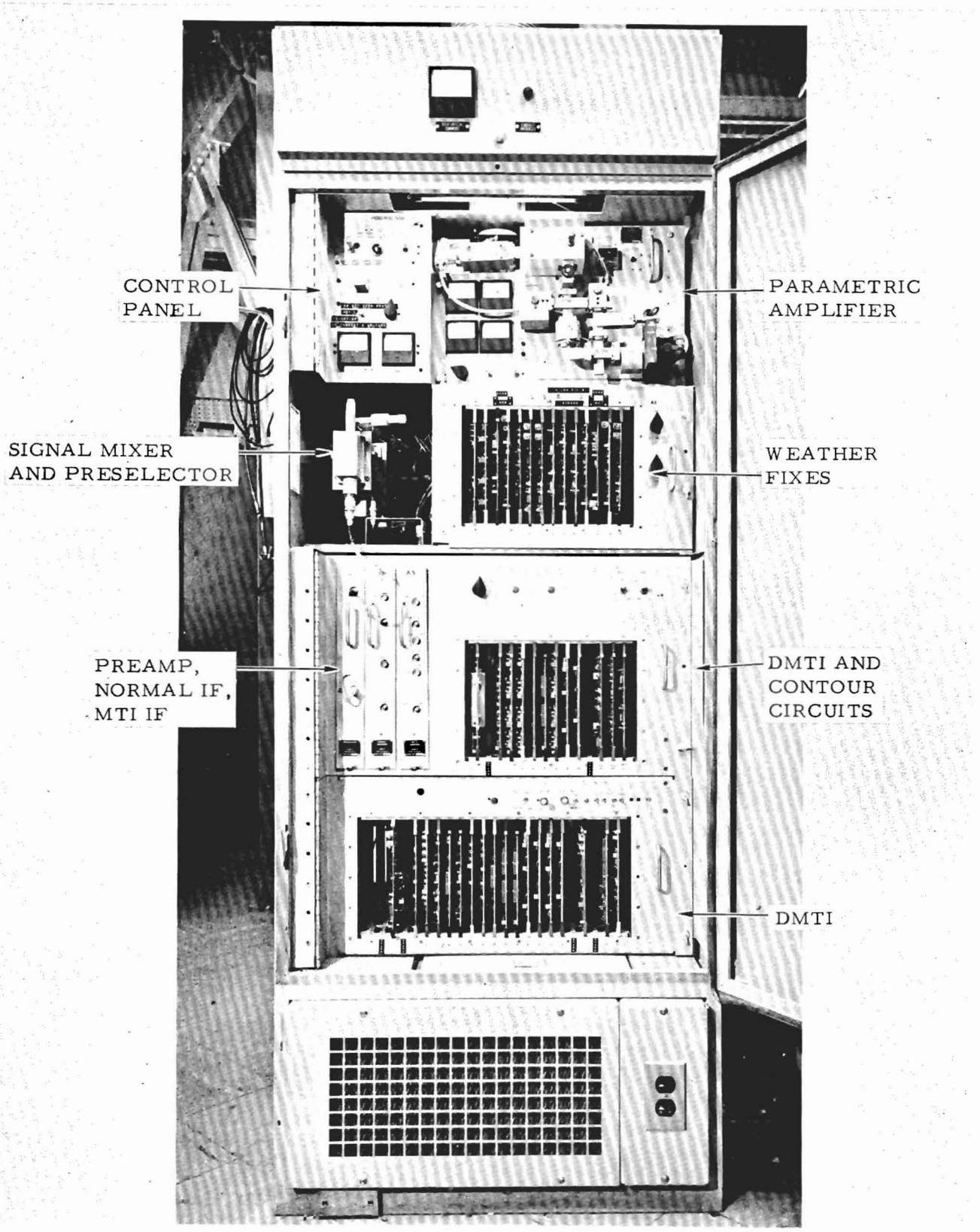

FIGURE A-1. WEATHER CLUTTER FEASIBILITY MODEL EQUIPMENT

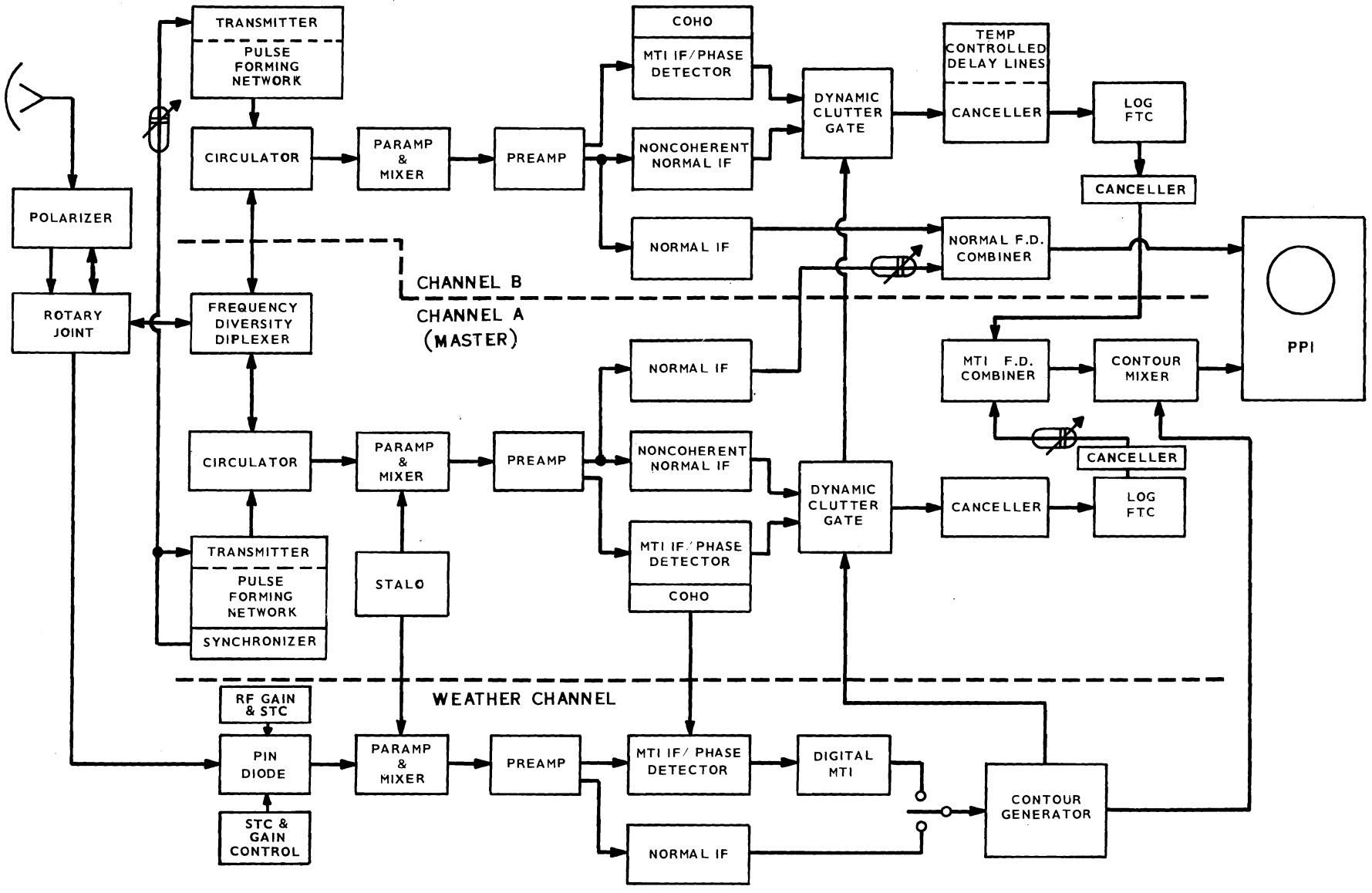

FIGURE A-2. WEATHER CLUTTER FEASIBILITY MODEL SIMPLIFIED BLOCK DIAGRAM

COHERENT OSCILLATOR.

The coherent oscillator energy for the contouring channel was also derived from channel A. To accomplish this, the channel A coherent oscillator output was routed to the weather channel cabinet. There it was split and amplified by two 30-MHz IF amplifiers. Each amplifier was controlled by a level-control potentiometer to furnish the desired inputs to the moving target indicator (MTI) IF amplifiers of the ASR-5 channel A and of the weather channel.

TEMPERATURE CONTROLLED DELAY LINES.

In order to operate in frequency diversity, the two ASR-5 channels must be synchronized. This was accomplished by slaving the master trigger of channel B to that of channel A. The heating of the channel B delay lines was made a function of the difference between the two-channel trigger times. Thus, as the timing of channel B varied from its nominal value of occurring 1 μs after channel A trigger, the temperature of the channel B delay lines was increased or decreased in such a manner as to bring the triggers back to proper timing. The error-sensing circuitry was located in the weather channel cabinet. It converted an error in system timing to a voltage which was added to the voltage on the channel B delay line heater to correct the error.

WEATHER CHANNEL RECEIVER.

The weather channel receiver is shown in figure A-2. The various portions of the receiver are discussed below.

PIN DIODE. The PIN diode was used as a microwave attenuator gain control device. It adjusted the level of the radiofrequency signal without affecting the receiver noise level. This provided the capability of reducing large clutter signals to below input saturation level. Five attenuation levels could be preset and selected either locally or remotely for receiver gain control. A maximum attenuation of 40 dB could be provided by the PIN diode. One of four adjustable STC curves from the weather channel STC unit could be also applied to the PIN diode.

BASIC RECEIVER. The ASR-7 type parametric amplifier, preamp, normal IF amplifier, and MTI IF amplifier made up the weather channel receiving system. An ASR-7 digital MTI canceller was also included to provide cancellation of fixed targets prior to contouring.

CONTOUR GENERATOR. The contour generator consisted of a log video amplifier, a level detector, and a contour-generating circuit. The output of the receiving system was applied to the log amplifier. This output could be selected to be normal video, MTI video, or range-gated MTI/normal video. The log video was then sent to the level detector. The level detector was a dual-channel pulse-height discriminator. Two channels were necessary to provide the desired two levels of contouring. Each channel contained a thresholding circuit in which the level of video to be contoured was set by potentiometers. The

contour-generating circuits produced weather contours from the two thresholding circuit outputs. These contours indicated the width of portions of the clutter which had intensities above the selected threshold values. A weather clutter gate and a video-blanking gate were also generated by this assembly. The clutter gate was used to switch the dynamic clutter gates for display of noncoherent MTI as discussed below. The video-blanking gate inhibited target video for a period before, and after weather contour video was applied to the display. Remote and local control of contour intensity was provided.

RANGE INTEGRATOR. The range integrator utilized capacitive integration to smooth out the weather-channel video prior to the generation of contours. This resulted in more regular and better defined contouring.

DYNAMIC CLUTTER GATES. The dynamic clutter gates were essentially single-pole, double-throw analog switches which passed one of two video input signals. The video selected depended on the logic state of the weather clutter gate line from the contour generator in the automatic mode or by manual selection in the manual mode. As seen in figure A-2, these two video inputs were coherent MTI from the ASR-5 MTI IF amplifier and noncoherent MTI from the noncoherent IF amplifier. During periods of weather clutter, noncoherent IF video was gated in by the automatic gating from the contour generator. For test purposes, the clutter gate could be operated in the manual mode with either coherent or noncoherent video selected for continuous display.

LOGARITHMIC FAST TIME CONSTANT (LOG/FTC). The log/FTC consisted of an integrated log circuit (SN 55502) to provide video log amplification, a delay and subtract FTC circuit, and an antilog circuit. The drive to the log amplifier provided approximately 20 dB of noise above the beginning of the log characteristic. This provided the CFAR action of the receiver. The log circuit was followed by the fast time constant circuit which consisted of an integrator, delay line, and subtractor. Long-duration signals (clutter) developed a mean value voltage in the integrator. This mean value, when combined with the delayed video in the subtractor, caused cancellation of the mean value of the clutter. Target signals, being of a short duration when compared to the time constant of the integrator, did not develop a significantly large mean value component in the integrator, and subtraction was not realized. The resulting video was then sent to the antilog circuit for signal-to-noise restoration.

FREQUENCY DIVERSITY COMBINERS. Figure A-2 shows the location of the frequency diversity combiners in the equipment. Normal and MTI combiners were provided. Channel A and channel B videos were applied to the combiners with the former being delayed 1 μs in delay lines to compensate for the 1 μs delay in channel B transmitter time. Each combiner functioned in the additive and multiplicative modes. In the additive mode, the signals from the two radar channels were summed. In the multiplicative mode, the product of the inputs was formed.

CONTOUR MIXER. The contour mixer was identical to the clutter gates discussed above. It functioned to combine the frequency diversity MTI video with the contour video from the contour generator for application to the system PPI. Contour video was automatically gated in by signals from the contour generator.

APPENDIX B

EQUIPMENT MODIFICATIONS

The following areas of operation were determined to be unsatisfactory during the evaluation period, and modifications were made as discussed below.

NONCOHERENT MTI.

The clutter-gating circuitry was activated by target signals causing targets in the clear to be displayed with noncoherent MTI. This resulted in the loss of targets. As discussed below, under weather channel modifications, increasing the weather-contouring range integrator time constant to avoid contouring (and consequently noncoherent gating) of targets resulted in contour stretching. Therefore, a target discriminator circuit was installed in the contour generator to inhibit any signal of less than 5 μs duration (one digital MTI range bin) from being contoured. With this modification, installed targets in the clear were displayed with coherent MTI.

LOG/FTC.

Operation of the log/FTC circuitry was determined to be unsatisfacory for several reasons, and modifications were performed as follows:

1. As originally configured, the log/FTC input was derived from the ASR-5 cancellers at J7209 (unipolar video after amplification and limiting). The system dynamic range at this point was approximately 15 dB, due to the limiter action. This reduced dynamic range was not suitable for log/FTC operation. Also, the capacitive coupling employed in the canceller video amplification and limiting circuits caused baseline shifting when heavy weather signals were present. This rendered the log/FTC inoperable since it was very sensitive to slight voltage changes. To correct these problems, the system cabling was changed to derive the log/FTC input from the output of the canceller bipolar to unipolar converter. At this point, the full MTI system dynamic range was available. Also, the log/FTC was direct-coupled to the canceller resulting in a greatly reduced baseline shift. An emitter follower circuit was installed to provide the necessary drive for the new cabling arrangement.

2. As originally configured, the wiper arm of the potentiometer in the emitter follower output of the log amplifier card was connected to the integrator and delay line portions of the fast time constant subtractor. Signals entering the delay line were integrated by the combination of the potentiometer resistance as adjusted and the integrator capacitance. This resulted in loss of signal strength out of the subtractor. The circuit was modified by replacing the potentiometer with an equivalent value resistance and connecting the fast time constant input directly to the transistor emitter. Gain control was maintained by reinstalling the potentiometer in the emitter followers base circuit.

3. The subtractor circuit originally employed a 2.3 μs fixed delay line. With this delay, target integration residue from the integrator leg of the subtractor was partially coincident with target signals from the delay line output. In the subtraction process, this residue caused partial loss of the target signals. To correct this problem, the fixed delay line was replaced with a variable delay line. This permitted adjusting the delay time for optimum signal strength out of the subtractor.

4. One cause of poor CFAR action was bottom clipping of signals and noise by the diodes of the unipolar to bipolar converters in the ASR-5 cancellers. A positive bias was placed on the anodes of the diodes, thereby lowering the forward voltage drop. This reduced the bottom clipping and consequently allowed better CFAR action.

5. As originally configured, the negative supply voltage circuit to the log input amplifiers contained an RC filter. When long-duration clutter signals were amplified, the filter caused a voltage shift of up to 200 mV at the log amplifier input. This shift rendered the log/FTC equipment inoperable. The resistive portion of the filter was removed improving the circuits voltage stability.

FREQUENCY DIVERSITY.

The output of the frequency diversity combiner had a greater signal-to-noise ratio than the input. This was due to the decorrelation effect of frequency diversity operation on random signals, such as system noise. This was especially true for operation in the multiplicative mode resulting in the possibility of exceeding the dynamic range of the PPI as the gain of the combiner was increased. To correct this situation, a limiter was incorporated at the outputs of the combiners to limit their output at 2 volts.

WEATHER CHANNEL.

The weather channel contoured target signals unless the range integrator had a sufficiently large time constant to inhibit it from doing so. This large time constant, however, also resulted in delay of contour presentation with respect to the clutter being contoured. To correct this problem, an inhibit gate was added to the contouring circuitry. This gate prevented any signal of less than 5 μs (1 digital MTI range bin) from entering the contour circuits. This permitted using less range integration and, consequently, allowed more accurate contouring.

Also, the range integrator was moved from the input to the output of the log amplifier portion of the contouring circuit. Charging of the integrator circuit was dependent on both signal amplitude and duration. Since the log amplifier standardized signal amplitudes, this change made the trailing edge contour position relatively independent of clutter signal amplitude.

APPENDIX C

SPECIAL TEST EQUIPMENT

Three special test equipments in the NAFEC ASR-5 test facility were utilized during this project. They were: a radiofrequency target generator, a noise source, and the radar data measuring system (RDMS).

The target generator was used to generate S-band ring-around and azimuth-gated (antenna scan modulated) targets. These signals were fed into the ASR-5 channel A system via the directional coupler. Controls on the unit permitted selection of target range and azimuth, velocity, phase, intensity, and radial direction of movement.

The noise source provided a ring-around noise signal 140 μs in duration. The intensity of the noise could be adjusted from system noise level to approximately 40 dB in intensity.

The RDMS was used to provide a tracking gate for tracking and identifying a desired aircraft.